8-11-2020

Brain Functional and Structural Networks Underpinning Musical Creativity

Kiran Dhakal

Recommended Citation
Dhakal, Kiran, "Brain Functional and Structural Networks Underpinning Musical Creativity." Dissertation, Georgia State University, 2020.
doi: https://doi.org/10.57709/18627932

BRAIN FUNCTIONAL AND STRUCTURAL NETWORKS UNDERPINNING MUSICAL CREATIVITY

by

KIRAN DHAKAL

Under the Direction of Mukesh Dhamala, Ph.D.

ABSTRACT

Musical improvisation is one of the most complex forms of creative behavior, which offers a realistic task paradigm for the investigation of real-time creativity. Despite previous studies on the topics of musical improvisation, brain activations, and creativity, the main questions about the neural mechanisms for musical improvisation in efforts to unlocking the mystery of human creativity remain unanswered. What are the brain regions that are activated during the improvised performances of music? How do these brain areas coordinate activity among themselves and others during such performances? Whether and how does the brain connectivity structure encapsulate such creative skills? In attempts to contribute to answering these questions, this dissertation examines the brain activity dynamics during musical

improvisation, explores white matter fiber architecture in advanced jazz improvisers using functional and structural magnetic resonance imaging (MRI) techniques. A group of advanced jazz musicians underwent functional and structural magnetic resonance brain imaging. While the functional MRI (fMRI) of their brains were collected, these expert improvisers performed vocalization and imagery improvisation and pre-learned melody tasks. The activation and connectivity analysis of the fMRI data showed that musical improvisation is characterized by higher brain activity with less functional connectivity compared to pre-learned melody in the brain network consisting of the dorsolateral prefrontal cortex (dlPFC), supplementary motor area (SMA), lateral premotor cortex (lPMC), Cerebellum (Cb) and Broca's Area (BCA). SMA received a dominant causal information flow from dlPFC during improvisation and prelearned melody tasks. The deterministic fiber tractography analysis also revealed that the underlying white matter structure and fiber pathways in advanced jazz improvisers were enhanced in advanced jazz improvisers compared to the control group of nonmusicians, specifically the dlPFC - SMA network. These results point to the notion that an expert's performance under real-time constraints is an internally directed behavior controlled primarily by a specific brain network, that has enhanced task-supportive structural connectivity. Overall, these findings suggest that a creative act of an expert is functionally controlled by a specific cortical network as in any internally directed attention and is encapsulated by the long-timescale brain structural network changes in support of the related cognitive underpinnings.

INDEX WORDS: Brain Activity, Functional Magnetic Resonance Imaging (fMRI), Diffusion Weighted Magnetic Resonance Imaging (DW-MRI), Diffusion Tensor Imaging (DTI), Blood-Oxygen-Level-Dependent (BOLD), Functional Connectivity (FC), Granger Causality (GC), Fiber Tractography, Deterministic Fiber Tracking, Fractional Anisotropy (FA), Quantitative Anisotropy (QA)

BRAIN FUNCTIONAL AND STRUCTURAL NETWORKS UNDERPINNING MUSICAL CREATIVITY

by

KIRAN DHAKAL

A Dissertation Submitted in Partial Fulfillment of the Requirements for the Degree of

Doctor of Philosophy

in the College of Arts and Sciences

Georgia State University

2020

BRAIN FUNCTIONAL AND STRUCTURAL NETWORKS UNDERPINNING MUSICAL CREATIVITY

by

KIRAN DHAKAL

Committee Chair: Mukesh Dhamala

Committee: Martin Norgaard

Brian D. Thoms

Douglas R. Gies

Vadym Apalkov

Electronic Version Approved:

Office of Graduate Services

College of Arts and Sciences

Georgia State University

August 2020

DEDICATION

To my loving parents, brother Keshav Dhakal
Caring wife Swikriti
And my beautiful daughters Aatmika and Advika

ACKNOWLEDGEMENTS

I am deeply indebted to many wonderful people who have supported me during my graduate study and research for a Ph.D. First and foremost, my sincere thanks go to my Ph.D. supervisor Dr. Mukesh Dhamala, who provided me enormous opportunities in the research field of my interest. He motivated me and put in a lot of effort and his invaluable expertise being available for extensive discussions. It would not have been possible to write this thesis without his endless help, support, and patience. I would like to acknowledge Dr. Martin Norgaard for always being so generous and for his expertise and precious time. I am very grateful to my dissertation committee members and all the members of the Neurophysics Research Group.

I would like to extend my sincere thanks to Dr. Xiaochun He, Dr. Mike Crenshaw, Dr. Brian D. Thoms, Dr. Murad Sarsour, Dr. Andrew J. Butler, and the department chair Dr. Sebastien Lepine, for their support and invaluable suggestions. I am very thankful to the Brains and Behavior (B&B) program at Neuroscience Institute for supporting me with B&B Fellowship & B&B travel awards. Also, I would like to thank GSU Study Abroad Program for awarding international education scholarship two times, which provided excellent opportunities not only to learn and explore the cutting-edge research and culture abroad but also to share our research with the international audience.

A big thanks go to my parents for their love and support throughout my life and for giving me the strength to chase my dreams. Also, I am very grateful to my brother Keshav Dhakal who supported me in all my pursuits. My special thanks to my loving wife, Swikriti, for all her devotion and love. Her sacrifices and encouragement throughout my career are truly undeniable. Finally, I would like to thank all the beautiful people, families, friends, and relatives who inspired and always supported me towards my graduate studies.

TABLE OF CONTENTS

LIST OF TABLES

LIST OF FIGURES

LIST OF ABBREVIATIONS

BA	Brodmann Area
BCA	Broca's Area
BOLD	Blood Oxygen Level Dependent
Cb	Cerebellum
DCM	Dynamic Causal Modeling
DICOM	Digital Imaging and Communications in Medicine (Image format)
dlPFC	Dorsolateral prefrontal cortex
DMN	Default Mode Network
DT	Diffusion tractography
DTI	Diffusion Tensor Imaging
DWI	Diffusion Weighted Imaging
ECN	Executive Control Network
EEG	Electroencephalography
FA	Fractional Anisotropy
FC	Functional Connectivity
FDR	False Discovery Rate
fMRI	Functional Magnetic Resonance Imaging
FWE	Family Wise Error
GC	Granger Causality
GFA	Generalized Fractional Anisotropy
GLM	Generalized Liner Model
GQI	Generalized Q-sampling Imaging
IFG	Inferior Frontal Gyrus
II	Imagine improvised
IMG	Imagine (Overall)
IMP	Improvisation
IP	Imagine prelearned

L	Left
LPM	Lateral premotor cortex
M	Male
MFG	Middle frontal gyrus
MNI	Montreal Neurological Institute
MR	Magnetic resonance
NIFTI	Neuroimaging Informatics Technology Initiative (Image format)
NQA	Normalized Quantitive Anisotropy
PAC	Primary Auditory Cortex (A1)
PL	Prelearned
PMD	Dorsal Premotor Cortex
PrCG	Precentral Gyrus
QA	Quantitive Anisotropy
QSDR	Q-Space Diffeomorphic Reconstruction
R	Right
RCB	Right cerebellum
ROIs	Regions of Interest
SC	Structural Connectivity
SMA	Supplementary motor area
STG	Superior Temporal Gyrus
TE	Echo Time
TIP	Topology-Informed Pruning
TR	Repetition Time
VI	Vocalize improvised
VOC	Vocalize (Overall)
VP	Vocalize prelearned

1 INTRODUCTION

1.1 Overview

Creativity, in general, is defined as an ability to create or generate something novel that is meaningful and valuable. From everyday situations to the pinnacles of science, creativity is seen as the ultimate ability that allows individuals to solve problems they have not encountered previously. Expert creativity is an extreme ability, predominantly shaped with domain-specific skills, experience, and strategies, also involve the domain-general ideas and responses. Experts are people who can produce exceptional performances even in new situations or complex environments, find and fix their cognitive limitations, and execute new strategies quickly and more effectively than novices [1]. Creative behaviors that unfold the expert's outstanding performances can take many forms in many domains, from sports, arts, diverging thinking, problem-solving to music. Specific examples include the unique movements of an expert basketball player bypassing defenders from the opposing team, the actual wording of a professional presenter using an outline, or the musical improvisation of an advanced jazz saxophonist who can continuously create and play new melodies.

Creative behaviors within the real-time constraints add not only the cognitive complexity but also demand online information processing, spontaneous production, and prompt execution and monitoring. These creative behaviors may be guided by larger consciously chosen goals (i.e., dunking the basketball), yet individual lower-level actions in support of those goals may happen so quickly that conscious evaluation is impossible (i.e., weaving past unforeseen opponents on the court). The lower level actions depend on an automated, yet flexible process developed through experience. The skilled speaker can seamlessly incorporate audience questions without hesitation, just like the expert basketball player can bypass defenders from the opposing team.

Through experience and practice, a collection of effective responses to environmental cues are stored in procedural memory. Inefficient or incorrect responses are culled, and successful responses remembered. This builds up a set of particular cues that trigger automated responses. This automated process, not dependent on conscious evaluation, has traditionally been thought of as inflexible. However, recent research indicates that it is possible to generate novel responses below consciousness if these responses are guided by specific goals [2]. Indeed, the expert jazz improviser sometimes plays material never played before, just like the basketball player may suddenly invent a new move without conscious contemplation. How this stored information is used and manipulated in real-time is still poorly understood.

Recent creativity studies have employed neuroimaging methods to explore the underlying neural basis of creativity in different domains. Although the findings suggest some common and distinct activations patterns across domain-specific and domain-general creative behaviors, including music, drawing, dance, and writing [3], how expert creativity reflects on brain activity and network connectivity is largely unknown. Further, how the neurocognitive mechanisms of expert creativity vary during constrained performances and free, spontaneous artistic performances and how such skills are facilitated by the underlying white matter fiber architecture is not well understood. Here, in our study, we incorporated the jazz musical improvisation to investigate the neuronal correlates of creativity in advanced level jazz improvisers, while being in the fMRI recording, improvisers performed improvisatory vocalization and imagery tasks. And, using diffusion weighted MRI, we examined the underlying white matter fiber properties of advanced jazz improvisers and compared the findings with the control group of nonmusicians.

1.2 Brain Imaging: Modalities and Measurements

The human brain is a complex and highly dynamic biological system made up of more than 100 billion nerves that communicate and coordinate with the body system for the proper organized functioning. It consists of around 100 billion neurons, the cells that transmit information inside the brain [4]. A typical neuron possesses three different parts; dendrites, the cell body (or soma), and the axon. The dendrites propagate the electrochemical stimulation received from other neural cells to the cell body or soma, the soma contains the nucleus and maintain the cell and keep the neuron functional, whereas the axon, the elongated fiber that extends from the cell body to the terminal endings, often covered with myelin, and transmits the neural signal [5-9]. On a larger scale, the human brain is divided along the middle into left and right interconnected hemispheres and consists of three main parts: cerebrum, cerebellum, and brainstem. All large-scale brain functional activities and structural changes can be influenced by the action potential firing in axons [7]. Brain functional and structural imaging adds new insight into our understanding of the origins of human cognition and skill development

Recent advancements in neuroimaging technology have provided state-of-the-art methods on understanding the brain mechanisms for behaviors, including human creativity. This dissertation describes the brain functional and structural networks underpinning musical creativity based on the study of advanced jazz improvisers in neuroimaging experiments. Neuroimaging data were collected using a magnetic resonance imaging (MRI) scanner with a field strength of 3.0 Tesla, which is around 60,000 times stronger than the earth's magnetic field. We used the blood-oxygenation level-dependent (BOLD) contrast-based functional MRI (fMRI) technique to study the brain functional network activity and connectivity, and the diffusion-

weighted MRI (DW-MRI or dMRI) to study the brain's structural network, white matter fiber architecture. Both imaging modalities are non-invasive brain imaging methods.

The biological tissue of our body, including the brain, consists of water molecules containing two hydrogen atoms and one oxygen atom. Each hydrogen atom has a single proton in its nuclei and acts as a tiny magnet that spins around its own magnetic axis. In the presence of the strong magnetic field inside the MRI scanner, randomly spinning hydrogen protons align themselves along the magnetic field, resulting in the net magnetization in the direction of the magnetic field, which becomes the source of MR image production [8, 9]. These hydrogen-protons in a magnetic field can absorb and transmit energy at the specific processional frequency, known as Larmor frequency [8, 9]. By applying a radio frequency (RF) pulse at Larmor frequency, the net magnetization will be tipped out of normal alignment, causing protons to shift their state that results in the transverse magnetization. After the RF excitation, protons release absorbed energy resulting in the net magnetization recovery to its aligned position with a spin-lattice relaxation process called T1 relaxation. Over time, the dephasing of protons caused by spin-spin interactions (T2 relaxation) results in the signal loss in the receiver coil. Further, the magnetic inhomogeneities contribute to faster dephasing of spins. The relaxation time due to the combination of all dephasing influences is called T2* relaxation and is the basis of the fMRI signal [9].

Functional MRI is an indirect measurement of the local neuronal activity by detecting the changes in blood oxygenation over time in the area of the brain is in use. The fMRI images are based on this physiological contrast of blood dependency and thus termed as "blood-oxygen-level-dependent" (BOLD) signal or bold contrast imaging [9, 10]. The regional blood oxygenation level changes can be attributed to the overall changes in the synaptic input to the

neuronal population of that region and its intrinsic processing [11, 12]. A combined effect of the energy demand and vascular changes following a neuronal activity leads to an oversupply of oxygen via oxygen-rich blood flow to the region, thus increasing the MR signal intensity [9, 13].

In addition to T1 and T2 imaging for anatomical structure, white matter fiber pathways can be mapped with diffusion MRI using the diffusion properties of water molecules in biological tissue. Diffusion weighted imaging is based on the random Brownian motion of water molecules in tissue and provides insight into the microscopic details of tissue architecture and white matter fiber tracts [14-16]. Diffusion MRI allows for spatial mapping of the diffusion signals [16, 17], by combining the pulse-gradient spin-echo (PGSE) sequence [18] and the spatial mapping of the diffusion coefficients [19]. Different local tissue structures and the molecular organization have different effects on the water diffusion dynamics, resulting in the hindered and restricted diffusion in the presence of biological barriers and free diffusion without any boundaries and barriers [9, 20]. Brain white matter structure has coherent fibrous architecture; thus, it will allow diffusion in one direction resulting in highly anisotropic measures, whereas water diffuses isotropically in less coherent structures like grey matter. Such anisotropic diffusion becomes a key measure in diffusion tracking, which has shown sensitivity for the study of white matter connectivity, integrity, and development, and reveals the fiber architecture, the trajectories, and the axonal directions [13, 14, 16, 21-31].

1.3 Structure of the Dissertation

Chapter 2 includes a brief description of network connectivity measures and fiber properties. Chapter 3 contains the details about functional MRI investigation of the advanced jazz improvisers. I will describe the study design, data collection procedure, data preprocessing and

analysis, and discuss our findings of the functional network, brain activity, and connectivity dynamics during musical improvisation and prelearned conditions.

Chapter 4 includes the diffusion weighted MRI investigation of the advanced jazz improvisers and the control group of nonmusicians. I will discuss our findings of the brain's structural network, white matter fiber architecture, and diffusion properties in advanced jazz improvisers compared to nonmusicians.

Chapter 5 summarizes the main conclusions of these studies.

This dissertation is based upon the following first two works in the list:

1. Dhakal K, Norgaard M, Adhikari BM, Yun K, and Dhamala, M. "Higher Brain Activity with Less Functional Connectivity during Musical Improvisation" DOI:10.1089/brain.2017.0566 Brain Connect 9: 296-309 (2019)
2. Dhakal K, Norgaard M, and Dhamala M. "Enhanced White Matter Fiber Tracts in Advanced Jazz Improvisers." NeuroImage (Under Review)
3. Dhakal K, Norgaard M, and Dhamala M. "Whole-brain functional connectivity during musical improvisation." (In preparation, 2020)

2 CONNECTIVITY MEASURES AND FIBER PROPERTIES

2.1 Directed connectivity measures

Brain connectivity analysis is widely used in neuroscience with neuroimaging data to infer the brain's functional and structural organization. Undirected functional connectivity measures include symmetry measures, such as pairwise correlation, ordinary coherence spectra, phase synchronization index, to tell us how different brain regions are functionally dependent on

each other. Asymmetric measures, such as Granger Causality and dynamical causal modeling (DCM) based coupling, can tell us about causal influences from one region to another region in the brain.

Granger Causality (GC) [32] and Dynamic Causal Modeling (DCM) [33] are the two most predominantly used methods on exploring the directional connectivity measures using functional neuroimaging. Although both methods have their own merits and demerits, one of the key differences between them is GC considers dependencies among measured responses, whereas DCM relies on probabilistic graphical modeling. In this work, we used GC analysis to uncover the patterns of information flow among the brain regions of interest (ROIs).

Granger causality (GC) is based on Wiener's idea of linear prediction, using autoregressive modeling of time series [34]. It was put forward with practical implementation by Clive W.J. Granger in 1969, who was a recipient of the 2003 Nobel Prize in Economics. For two simultaneously measured time series such as **1:** $X_1(1)$, $X_1(2)$, ……, $X_1(t)$, ……, and **2:** $X_2(1)$, $X_2(2)$, ……, $X_2(t)$, ……, Granger causality can be estimated using either autoregressive modeling (parametric methods) or by using direct Fourier or wavelet transforms (nonparametric) spectral decomposition approach [35-37]. We can obtain the noise covariance matrix (Σ), the transformation function ($H(f)$), and the spectral density matrix ($S(f)$) from these time series, such that $S(f) = H(f)\,\Sigma\,H^*(f)$. The noise covariance matrix (Σ) is computed from the residual errors of the prediction models, and the transfer function H is obtained from the matrix inverse of the Fourier transforms of the coefficients in the prediction models. For non-stationary process, S, H, and Σ can be estimated using the wavelet transforms-based non-parametric estimation [35, 36], so that these quantities become the function of both time and frequency domains.

The spectral GC from 2 to 1, $M_{2\to1}(f)$ can be obtained as

$$M_{2\to1}(f) = -ln\frac{S_{11}(f)-\left(\Sigma_{22}-\frac{\Sigma^2_{12}}{\Sigma_{11}}\right)|H_{12}(f)|^2}{S_{11(f)}} \quad (2.1)$$

where, by interchanging 1 and 2, one can compute the spectral GC from 1 to 2, $M_{1\to2}(f)$. The time-domain Granger causality can be obtained by integration over the entire frequency range.

The total interdependency measures of statistically inter-related two non-stationary processes 1 & 2, consists of sub-measures and can be expressed as;

$$M_{1,2} = M_{1\to2} + M_{2\to1} + M_{1.2} \quad (2.2)$$

where $M_{2\to1}$ and $M_{1\to2}$ are one-way directional delayed causal flow from 2 to 1 and 1 to 2, and $M_{1.2}$ is non-delayed instantaneous causal flow.

2.2 Fiber properties

Diffusion weighted imaging (DWI), and fiber tractography are widely used tools to describe the underlying white matter diffusion properties and fiber integrity in health, development, and disorders. DWI is based on the random Brownian motion of water molecules, utilized to track the anisotropic diffusion mechanism corresponding to the white matter structure and fiber tracts. Several reconstruction methods are available to carry out fiber tracking, both model-based methods (parametric approach) and a model-free approach (non-parametric approach), with their strength and weakness.

The multi-tensor model [38], the ball-and-sticks model implemented in bedpost FSL toolbox [22], and neurite orientation dispersion and density imaging (NODDI) [39] model are commonly used model-based methods which consider a predefined diffusion distribution function or pattern. Although the model-based methods need a few samples, a complicated

model might lead to overfitting while getting the whole distribution [27]. The constrained spherical deconvolution (CSD) method implemented in the MRtrix toolbox is considered as a model-based and model-free approach that accounts for the fiber orientation distribution function (ODF). Still, the deconvolution depends on the signal response. The CSD methods may benefit from both model-based and model-free approaches; this suffers from model violation, model mismatch, and the false fiber crossing geometry [40, 41].

The diffusion spectrum imaging (DSI), q-ball imaging (QBI), and generalized q-sampling imaging (GQI) are widely used model-free methods. Since DSI and QBI methods only work on grid data, and shell data respectively, the GQI method which is adopted in DSI studio toolbox (http://dsi-studio.labsolver.org/) has the obvious advantage as this works perfectly for both grid data, shell data as well as multi-shell, and non-grid-non-shell data [27, 28, 42, 43]. Further, GQI quantifies the density of diffusing water, and the orientation distribution function (ODF) of diffusing spins can be measured in terms of spin distribution function (SDF), which has greater sensitivity and specificity to white matter characteristics and fiber pathology [27, 28]. The q-space diffeomorphic reconstruction (QSDR) implemented in DSI Studio reconstructs the GQI diffusion pattern directly in the standard neuroimaging template, thus enabling template construction, connectome fingerprints, and connectometry analysis to get density-based measurements such as Quantitative Anisotropy (QA), rather than Fractional Anisotropy (FA). The FA measurement is a voxel-specific diffusion index shared by all-fiber population within a voxel, which is estimated using diffusion tensor imaging probabilistic tracking, a method that relies on the movement of water molecules (i.e., diffusivity, how fast water molecules move along axonal fiber tracts) [14, 15]. On the other hand, QA measurement is a fiber-specific diffusion index specific to each fiber population, which is calculated using the peak orientations

of the spin distribution function, which quantifies the diffusion density of water molecules along the fiber tracts [27]. QA is reported to have lower susceptibility to partial volume effects of crossing fibers and free-water, resulting in a better resolution with QA-aided tractography, which is known to outperform the FA-aided tractography [28, 44]. In our diffusion MRI investigation (explained in chapter 4), we used the DSI Studio toolbox that has adopted the GQI approach, QSDR reconstruction, and QA-aided deterministic fiber tractography.

3 BRAIN ACTIVITY AND FUNCTIONAL NETWORK INTERACTION

3.1 Introduction

Musical improvisation is an excellent model to study human creativity in which the output is created in real-time and revision impossible. Similar to innovative verbalizations or movement sequences, musical improvisation is only possible because choices are constrained by stylistic rules and physical limitations [45]. Expert practitioners who have internalized these rules and practiced the related motor movements can produce amazingly intricate improvisations. Despite some previous studies, the neural underpinnings of expert's improvising performance; what and how brain areas are involved during musical improvisation are not clearly understood. Here, we designed a new functional magnetic resonance imaging (fMRI) study, in which, while being in the MRI scanner, advanced jazz improvisers performed improvisatory vocalization and imagination as main tasks and performed a pre-learned melody as a control task. We incorporated an imaginary musical task to avoid possible confounds of mixed motor and perceptual variables in previous studies.

This spontaneous process may involve divergent brain activation and connectivity patterns. One emerging idea is that creative behavior, such as musical improvisation, involves

the dynamic interaction of the default mode network (DMN) and the executive control network (ECN)[46]. Interestingly, these two networks are usually associated with different tasks and are typically not active concurrently. DMN activity is associated with spontaneous and self-generated thought, including mind-wandering, mental stimulation, social cognition, autobiographical retrieval, and episodic future thinking whereas, ECN activity is associated with cognitive processes that require externally-directed attention, including working memory, relational integration, and task-set switching [46]. Improvisation may involve the interaction between an automatic bottom-up process (DMN) that may supply possible choices and a top-down control process (ECN) that may guide those choices according to hierarchical rules [47, 48].

3.1.1 Improvisers manipulate elements on different hierarchical levels

The hierarchical structure of tonal music is a central constraint that may be used by the ECN to evaluate and select choices offered up by the DMN. Musical events, henceforth referred to as notes, are organized into two independent hierarchical structures related to rhythm and pitch, respectively [49]. The lowest level of the rhythm hierarchy relates to distances in time between individual notes. Higher levels relate to note groupings. Meter refers to a rhythmic reference that typically is constant throughout large sections of music. For instance, in a musical piece in waltz meter, timings of individual notes are related to a rhythmic framework in which every third instance is emphasized. Similarly, pitches are organized hierarchically with the individual frequency distance between two notes referred to as an interval, small note groupings as motives, slightly longer groupings as phrases, and longer sections as choruses.

Koechlin and Jubault (2006) [50] suggested Broca's area (BCA) and its right homolog are specifically involved in the hierarchical organization of actions, whereas other areas in the

frontal lobe process temporal organization. Accordingly, “appropriate actions are selected as subordinate elements that compose ongoing structured action plans rather than from occurrences of temporally distant events” (p. 963). Specifically, Koechlin and Jubault (2006) predict that phasic activations are different for action selection on three hierarchical levels in a button-pressing task [50]. Premotor regions control the selection of individual motor movements while posterior BCA is engaged at the second level, the boundaries between simple action chunks (collection of basic information units). The third and highest hierarchical level could be defined as groupings of simple action chunks. Koechlin and Jubault showed experimentally that anterior BCA regions are specifically involved in the selection and inhibition of these action chunk groupings [50]. Recently, Alamia et al. (2016) showed that disruption to BCA by transitory application of transcranial magnetic stimulation inhibited participant’s ability to chunk nonmotor sequences [51].

Skilled improvisers manipulate elements within the tonal and rhythmic hierarchies to create and violate the expectations of the listener. On a lower level, improvisers may repeat motives or introduce tension by employing notes from outside the dominant tonality. On a higher level, improvisers describe organizing their entire solo around an architectural design [52, 53]. Independent of training, listeners within a musical culture learn to decode expectations and violations much the same way they learn their native language [54]. Furthermore, it appears that these fulfilled or violated predictions may elicit emotions in the listener [55, 56]. Listeners appear to prefer music that contains a balance of predictability and novelty as related to their individual background [57]. We would expect the involvement of BCA and other regions related to the ECN during musical improvisation as available choices has to be evaluated and selected according to these intricate hierarchical musical rules.

3.1.2 Improvisations consist of concatenated motor movements

One of the most cited theoretical frameworks for cognition behind improvisation is the Pressing's framework, which is centered around concatenated motor movements [45]. Indeed reviews of large corpora of jazz improvisations have identified numerous repeated musical patterns that more than likely are generated using corresponding motor chunks [58]. On a higher level, the motor chunks are likely selected according to higher-level plans for action chunk groupings [53]. Though Pressing's framework does not specifically include action chunk groupings, the verbal accounts of improvisers would appear to indicate that they often concentrate on this higher hierarchical level. In addition, experimental research shows that melodic patterns are more frequent in improvisations done while conscious involvement is attenuated through engagement with a secondary unrelated task [59]. This would indicate that less cognitive engagement with the improvisation inhibits the improviser's ability to vary and design improvisations around higher hierarchical plans, instead of relying on a smaller repertoire of repeated motor chunks. In other words, when a secondary task engages the ECN, the lack of control may result in the improviser using more stereotypical patterns offered up by the DMN.

3.1.3 Previous studies of musical improvisation used overt movement tasks

There is some support for the interaction between the DMN and the ECN during musical improvisation from previous neuroimaging research. However, much of this research used only pianists who performed supine in an MRI scanner on very short keyboards limiting ecological validity and generalizability to other instruments. Berkowitz and Ansari (2008) investigated neural correlates of musical improvisation in a study in which trained pianists played either novel or pre-learned rhythmic and melodic sequences while functional magnetic resonance imaging (fMRI) data were collected [60]. A brain network was identified based on activations in the

dorsal premotor cortex (PMD), the rostral cingulate zone of the anterior cingulate cortex, and the inferior frontal gyrus (IFG) during improvisation compared to pre-learned condition. However, the participants were classically trained pianists with no prior experience of jazz improvisation. Due to the lack of improvisational training, it is possible that the ECN was heavily engaged during this study as participants were grappling with the novel improvisational task. In addition, the musicians played on a keyboard with only five notes, severely limiting note choices.

Another study by Limb and Braun (2008) used a similar contrast and found that the entire dorsolateral prefrontal region was attenuated during improvisation, partially contradicting the activations found by Berkowitz and Ansari. Limb and Braun investigated brain activity while jazz pianists played either a pre-learned melody or an improvised solo over the same accompaniment [61]. The six participants in this study were advanced improvisers who were accompanied by a jazz rhythm track and played a 35-note keyboard. Limb and Braun concluded that conscious control processes are less active during improvisation and theorized that the medial prefrontal regions could generate the improvised output without conscious involvement. In this case, the DMN may have been able to guide improvisational choices due to the high level of improvisational training of the participants. Indeed, another study that included expert improvisers, and included interaction found increased activation in frontal control regions [62]. Here the extra cognitive resources related to interpreting and responding to another musician during improvisation may be responsible for the activation related to the ECN.

Manzano and colleagues investigated improvisations by a group of professional classical pianists, by studying overlaps and differences in brain activity during both pseudo-random key presses and piano improvisation [63]. The activity in both modes of generation was significantly higher in IFG, which included the dorsolateral prefrontal cortex (dlPFC), bilateral insula, and

cerebellum (Cb) compared to a control condition. They concluded the activation pattern reflects a generic process that is independent of the overall goal. Again, the activation of frontal control regions may have been related to the task of selecting novel keypresses, which is unfamiliar to classical pianists used to only performing pre-learned music.

To reconcile previous contradictory findings related to prefrontal control regions, a recent study by Pinho compared activation during an emotional play condition (play happy or fearful melody) with a pitch-set condition [64]. The pitch-set conditions (pitch-set vs. emotional) induced a comparably greater activation of the bilateral dlPFC, extending throughout the middle frontal gyrus into the PMD in the right hemisphere. In addition, there was greater activity in the bilateral parietal lobes. The reverse contrast (emotional vs. pitch-set) revealed comparably greater activation of the left dorsomedial prefrontal cortex in the superior medial gyrus, the left medial orbital gyrus, and bilateral insula, extending into the amygdala. They interpreted the results as suggesting the dlPFC activation during improvisation with a limited number of pitches is due to subjects holding the pitch-set in working memory. On the other hand, during the emotional condition, subjects relied on implicit associations between valence and musical output. Concerning connectivity, the emotional condition was associated with increased connectivity between dlPFC and the DMN. Beaty et al. (2016) suggested that the dlPFC may exert a top-down influence over generative processes stemming from the default network during the strategic expression of emotionally based improvisation [46].

3.1.4 Vocalizing and imagery improvisations

Participants engaged in overt motor movements in all previous studies. Though attempts were made to control variables, the current study bypassed potential confounds related to overt movement by including an imaginary task. It is well established that auditory perceptual and

secondary motor regions can be activated during covert auditory imagery. This effect has been observed during internal auditory discrimination [65], auditory imagery of a musical score [66], and even during passive listening [67]. In a study with advanced pianists, Meister et al. (2004) found a bilateral frontoparietal network was active during both play and imagery. The only difference was that during imagining activation in the contralateral primary motor cortex and bilateral posterior parietal cortex was not observed [68]. Interestingly, the level of motor activation is dependent on the subject's knowledge of the actual movements necessary to play the music even in listening only conditions, and this association can be trained over just a couple of days [69]. Finally, expert musicians often use mental imagery explicitly during both practicing and actual performance; for a review, please see Keller (2011) [70].

We investigated differences in activations between vocalizing and imagery pre-learned and improvised music. Specifically, the participants vocalized or imagined singing well-known melodies and continued to improvise over those melodies and the related chord structure. This task allowed for the recruitment of expert jazz improvisers who played several different primary instruments. We hypothesized that the improvisation minus pre-learned contrast would activate a network similar to networks identified in previous research related to music improvisation. This would include BCA in IFG, the dlPFC, premotor areas, parietal association areas, and the cerebellum. We also hypothesized that the contrast would include the BCA for the following reason: As the four included melodies were well-known, participants would more than likely have learned to combine related motor movements into larger chunks representing longer phrases of the melodies. On the other hand, improvisations would involve selecting and inhibiting unwanted motor chunks. Furthermore, during improvisation, those chunks may be selected according to architectural plans on a higher hierarchical level. We did not have predictions

related to changes in connectivity as earlier studies utilizing the contrast between improvisation and memory retrieval did not report related changes in connectivity. We did, however, hypothesize that the STG would be part of a network-based on our prior electroencephalography study [71] and the location of the auditory cortices.

3.2 Materials and Methods

3.2.1 Participants

Twenty-four male advanced jazz improvisers (4 left-handed, 20 right-handed; mean age ± standard deviation (sd)=31.9±13.6 years) were exclusively recruited for this study. A criterion for participation was expertise in jazz improvisation. Participants had at least six years of professional experience (mean ± sd=21.3±13.5 years) on jazz improvisation (see **Table 3.1**). Almost all the participants had previous education in a University System School of Music (n=23); average schooling years for all participants was 16.2 years (sd=1.8 years). Participants were also required to know how to read music. Primary instruments included piano (n=5), saxophone (n=11), guitar (n=2), trumpet (n=2), drums (n=1), trombone (n=1), French horn (n=1), and bass (n=1). All participants had normal or corrected to normal vision and reported normal neurological history. Participants provided written and signed consent forms and were compensated for their participation in the experiment. Institutional Review Board for Joint Georgia State University and Georgia Institute of Technology Center for Advanced Brain Imaging, Atlanta, Georgia, approved this study.

Table 3.1 Participants Musical Background and Demographic Data

Age, the primary musical instrument, and years of experience (Jazz Experience). Participants, shown in bold italic faces in the table, had all runs with improper timing duration during task performances and were excluded from the data analysis

Participant No.	***Age (Years)***	***Years of Experience (Jazz Improvisation)***	***Primary Instrument***
01	31	24	Piano
02	57	50	Piano
03	41	31	Saxophone
04	43	34	Piano
05	33	22	Piano
06	20	6	Guitar
07	***35***	***24***	***Saxophone***
08	22	10	Saxophone
09	26	15	Saxophone
10	41	33	Saxophone
11	***77***	***60***	***Saxophone***
12	23	11	Saxophone
13	19	10	Saxophone
14	26	18	Piano
15	30	18	Contra/Double Bass
16	21	12	Trombone
17	28	14	Drum Set
18	23	14	Saxophone
19	23	12	Saxophone
20	***23***	***7***	***French Horn***

21	42	33	Trumpet
22	38	28	Saxophone
23	***22***	***15***	***Guitar***
24	22	11	Trumpet

3.2.2 Experimental conditions

Prior to fMRI recording, participants were familiarized with the four tasks: Vocalize Pre-learned, Vocalize Improvised, Imagine Pre-learned, and Imagine Improvised. During the pre-learned conditions, participants were prompted to vocalize or imagine one of the four melodies (Au Privave, Now's the Time, Blues for Alice, and Billies Bounce) (**Figure 3.1 (A)**), which were memorized and rehearsed prior to the day of the experiment. All four melodies are based on a standard 12-bar blues chordal progression. And, participants were familiar with the melodies prior to the testing. In addition, they were tested on competency upon arrival. Participants were instructed to imagine singing during the imagery condition and to sing (vocalize) during vocalization. These four melodies were chosen from the Bebop era of jazz, as the complexity of these melodies is comparable to expected improvisations [52]. During Imagine Pre-learned condition, participants were instructed to imagine melodies without any overt vocalizations. These performances of pre-learned melodies from memory require little to no creativity. Results from both pre-learned conditions were contrasted with the two improvised conditions: Vocalize Improvised and Imagine Improvised, during which participants vocalized or imagined a spontaneously improvised melody over the blues chord progression. We did not require participants to vocalize melodies and improvisations at the quality of a trained jazz singer. Here, we simply asked the musicians to vocalize as they would during a practice session (non-wind

instrumentalists) or during casual practice without the instrument. Such practice is common among jazz musicians, and jazz students are typically asked to vocalize improvisations as a pedagogical tool [52].

No metronome beat was audible during the experimental conditions, but before each trial, there was an audible beat representing a two-measure count-in (for 3.6 s). Participants vocalized or imagined the cued melody twice and then went directly into a two-chorus improvisation over the same harmonic progression. Participants indicated that they switched from melody to improvisation by pressing a button.

Upon arrival at the testing site, participants provided informed consent and were familiarized with the task. They went through practice sessions at a mock scanner to reduce anxiety and make sure they performed all experimental tasks correctly prior to going into the scanner for actual functional runs. They were asked to remain still, not to move their heads or other parts of their body during the recording session. An fMRI compatible microphone was used for auditory recording. To constrain head motion, foam pads were used as support in the head coil. The task sequences were displayed in a screen inside the scanner via the E-prime program "E-prime_V2.0.10.242" (https://www.pstnet.com/eprime.cfm). All trials began with the instructional cue, followed by the two-measure audible count. After the count-in, participants were required to complete the cued task, at first performing the pre-learned melody twice and then the improvisation over two blues choruses. A button press preceded improvisation once participants performed the pre-learned melody twice. There was a rest period before the start of another trial, and during the rest period, participants were instructed not to do anything, remain still, and focus on the central crossbar on the screen. All trials followed the same structure over time (**Figure 3.1 (B)**) and were randomly selected with no repetition, so each run contained

vocalized and imagined trials of each of the four melodies. Each experiment was composed of 3 functional runs, with eight randomized trials in each run. Each functional had a 30 s rest period at the beginning and the end.

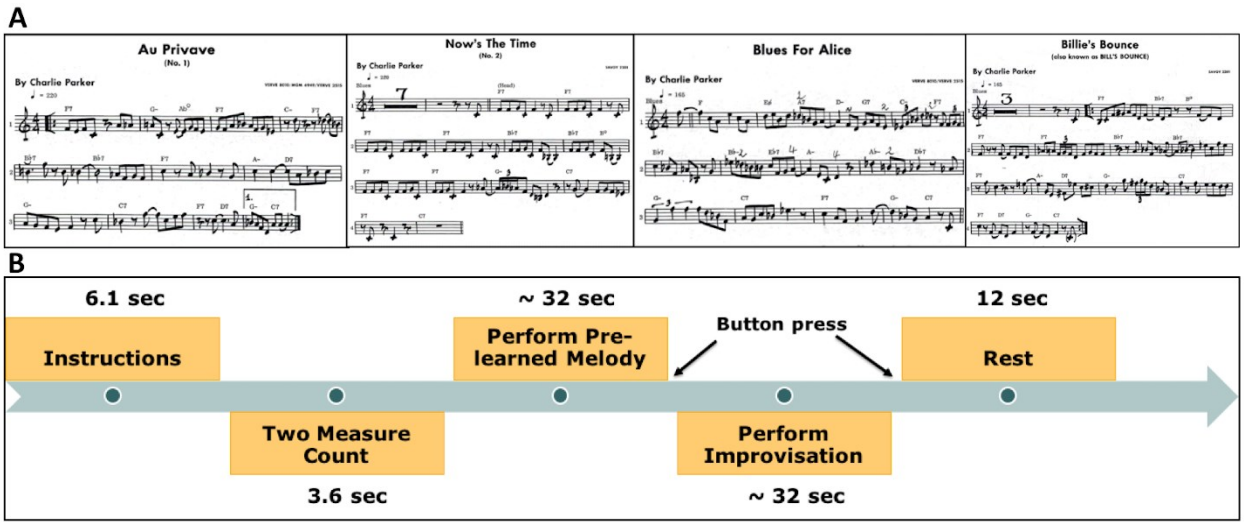

Figure 3.1 Jazz Melodies and experimental task paradigm

Four melodies (A): Au Privave, Now's the Time, Blues for Alice, and Billie's Bounce that were used in the experiment. (B) Task paradigm during a functional run; each functional run starts with initial 30 seconds rest followed by a task trial that included 6.1 seconds instructional cue that displays whether to vocalize or imagine a given melody, 3.6 seconds, two-measure count audio metronomes. Participants were instructed to press a response key inside the scanner after at the end of each task in a trial.

3.3 Data Acquisition and Analysis

3.3.1 Behavioral data analysis

Behavioral data were recorded on the computer that also ran the E-prime program displaying the experimental task sequences. The audio output (vocalized melodies and

improvisations) was recorded as MP3 files using an fMRI scanner compatible microphone. Stimulus onset time and the time between the onset of a condition and the button press (start of improvisation) in each trial were recorded. Audio files were analyzed to determine participants' performance accuracy in reproducing the cued melodies. The improvisations were evaluated to ensure they implied the dictated blues chord progression. Any performed conditions with improper timing (taking a long or short time duration) were not included in data analysis. Participants were excluded from further analysis based on improper trial durations. The average time duration for each trial was 32 s melody followed by a 32 s improvisation.

3.3.2 Functional magnetic resonance imaging (fMRI) data

The whole-brain MR imaging was done on a 3-Tesla Siemens scanner available at Georgia State University and Georgia Institute of Technology Center for Advanced Brain Imaging, Atlanta, Georgia. The functional scans were acquired with T2*- weighted gradient echo-planar imaging (EPI) sequence: echo time (TE)=30 ms, repetition time (TR)=1970 ms, flip-angle=90°, field of view (FOV)=204 mm, matrix size=68×68, voxel size=3×3×3 mm^3 and 37 interleaved axial slices with a thickness of 3 mm each. High-resolution anatomical images were acquired for anatomical references using a magnetization-prepared rapid gradient-echo sequence with TR=2250 ms, TE=4.18 ms, flip-angle=9°, voxel size=1×1×1 mm^3.

Functional MRI data were preprocessed by using Statistical Parametric Mapping (SPM12, Welcome Trust Centre, London, http://www.fil.ion.ucl.ac.uk/spm). The preprocessing steps involved slice timing correction, motion correction, co-registration to individual anatomical image, and normalization to Montreal Neurological Institute (MNI) template [72]. The spatial smoothing of the normalized image was done with an 8-mm isotropic Gaussian kernel. A random-effect, model-based, univariate statistical analysis was performed in a two-level

procedure. At the first level, a separate general linear model (GLM) was specified according to the task sequences. The conditions: rest, vocalize pre-learned, vocalize improvised, imagine pre-learned, and imagine improvised and six motion parameters were included in GLM analysis. The six motion parameters were entered as nuisance covariates and were regressed out of the data. Individual contrast images from the first-level analysis were then entered into a second-level analysis for a separate one-sample t-test, which gives brain activations for that condition versus baseline comparison condition. The resulting summary statistical maps were then thresholded and overlaid on high-resolution structural images in MNI orientation. The activation clusters were identified under the statistical significance $p < 0.05$, family-wise error (FWE) correction, for multiple comparisons correction and cluster extent $k > 20$; except in improvisation versus pre-learned contrasts with $p < 0.0005$ uncorrected FWE and cluster extent $k > 20$.

3.3.3 Network Connectivity analysis

The regions of interest (ROIs) were based on activation t-maps during overall improvisation (vocalize improvised+imagine improvised) compared to overall pre-learned (vocalize pre-learned+imagine pre-learned) condition except for primary auditory cortex in the temporal region, which is based on our hypothesis. We defined six ROIs, a sphere of 6 mm radius in MarsBar (http://marsbar.sourceforge.net/). The center coordinates were: (-54, 11, 17) for Broca's area (BCA) in inferior frontal gyrus (IFG), (-24, -10, 53) for the left lateral premotor area (lPMC) in middle frontal gyrus (MFG), (-9, 5, 68) for the left supplementary motor area (SMA), (30, -67, -22) for the right cerebellum (RCb), (-54, 11, 29) for the left dorsolateral prefrontal cortex (dlPFC) and (63, -10, 2) for the primary auditory cortex in superior temporal gyrus (STG). The time courses from all the voxels within each ROI and all subjects were extracted for the above-mentioned experimental task conditions. The ensemble-mean removed

segmented time series from separate voxels; task blocks (for stimulus on period only) and subjects were treated as trials for reliable estimates of the network measures.

3.3.4 Functional connectivity

Average time series for a trial was calculated for each subject from all ROIs. We then calculated pairwise correlation coefficients from trial to trial between two ROIs. To estimate the average effect, we used Fisher's z-transformation [73-75] on correlation values. The correlation values were converted to their equivalent Fisher's z-values ($z = \arctan h(r)$) and computed average Fisher's z-value. The average Fisher's z-values were then used to calculate the grand average z-value, the statistical significance level p, and the corresponding correlation coefficient for each pair of ROIs. Inter-regional correlation analysis was performed in overall musical improvisation and pre-learned and in vocalize and imagery conditions.

3.3.5 Directed functional connectivity

We performed the Granger causality (GC) analysis to characterize the directional information flow between ROIs. Blood oxygen level dependent (BOLD) signals are believed to originate from smoothing of neuronal activity by the hemodynamic response function [76, 77], we constructed hidden neural signals by hemodynamic deconvolution for each ROI data as suggested in previous studies [77-81] and used these deconvolved fMRI-BOLD time series for directed connectivity calculation. The ensemble-mean removed, segmented deconvolved time series from separate voxels and subjects were treated as trials for reliable estimates of the network measures. We calculated the frequency-dependent GC spectra [82] for pairs of ROIs. The significant GC spectra and hence the significant network interactions were defined by setting a GC threshold above the random-noise baseline. We constructed a set of surrogates by randomly permuting trial data from each participant and task condition. To compute the GC

threshold value, we used a random permutation technique [83, 84], and the threshold value was based on the null hypothesis that there was no statistical interdependence between nodes when trials were randomized. We computed GC spectra from all possible pairs of ROIs with a minimum of 1000 random permutations and picked maximum GC on each permutation. The threshold for GC spectra at significance $p<10^{-6}$ was obtained by fitting the distribution with a gamma-distribution function [35], and this threshold value was used to identify a significantly active directed network activity among ROIs. Conditional GC analysis was carried to rule out the mediated interactions among the ROIs and to retain only the direct network interactions. We also computed the time-domain GC values for significantly active network directions from each participant and performed paired t-tests on these values to find the significant network modulation during the various musical task conditions.

3.4 Results

3.4.1 Behavioral results

All recorded pre-learned and improvised vocalizations audio files were analyzed to assure the number of notes during the pre-learned and improvised conditions were not significantly different. A paired t-test found that there was not any significant difference in note count between the two conditions. Imagined tasks were monitored during recording, and later, recorded files were examined to make sure there were no confound vocalizations during imagined tasks. At the end of each recording session, participants reported that they performed the tasks as accurately as possible.

Any trial or session with improper behavior response time, either too long or too short response duration, was not included in data analysis. Trials were monitored during data

acquisition and compared to the expected length. Based on the tempo given by the metronome played at the beginning of each trial, vocalizing or imagining twice the improvisations or the melodies, should take about 32 s, so only the trials with durations between 28 s to 38 s were included in data analysis. Four participants (participant number: 7, 11, 20, and 23), shown in *bold italic* faces in **Table 3.1** had all sessions with improper response time duration and were thus excluded from fMRI data analysis. Excluding 4 participants resulted in the mean age (± standard deviation (std)) and mean years of experience (± std) from 31.9±13.6 years and 21.3±13.5 years to 30.9±13.3 years and 20.2±12.8 years respectively.

In addition, the vocalization trials were rated for accuracy independently by two expert jazz musicians not affiliated with the study using the Consensual Assessment Technique [85]. Accuracy was rated on a seven-point Likert Scale with 1 being "extremely inaccurate" and 7 being "highly accurate." Accuracy for the improvisation trials was defined as "pitches imply underlying blues chord progression and rhythms imply a steady pulse." We should note that due to technical difficulties, we only recorded the audio from 13 participants though vocalizations were monitored during the data acquisition. Mean ratings (± std) were 6.34 (±0.35) and 6.01 (±0.37) for the pre-learned and the improvised vocalizations respectively. **Table A.1.1** and **Table A.1.2** in the appendix include the subject wise and run wise rating details for improvised vocalization and prelearned vocalization, respectively.

3.4.2 Brain activations

Brain activations were studied with all possible contrasts: vocalize improvised (VI) versus vocalize pre-learned (VP), imagine improvised (II) versus imagine pre-learned (IP), overall improvisation (VI+II) versus overall pre-learned (VP+IP). Each of these tasks was also compared to the rest as a baseline. During each improvisational task, there was significantly

higher brain activation compared to pre-learned conditions, but there was no activation the other way around. The brain activations during any improvised or pre-learned tasks or any combination of tasks were always significantly higher when compared to rest, but no activation was observed when comparing rest to the other conditions. Significant brain activations are listed in **Table 3.2**.

Table 3.2 Brain Activations for various contrasts

The table includes information about the anatomical locations, cluster sizes, t-value (z-score), and MNI coordinates for brain activations during various contrasts. The brain activations listed in the table for contrasts compared with rest are under statistical significance $p<0.05$, FWE correction, for multiple comparisons correction, and cluster extent $k>20$. The brain activations that compare two task conditions are for $p< 0.0005$ (uncorrected FWE) and $k>20$.

Contrast	Cluster size	Brain region	Brodmann area	Voxel t (z-equivalent)	MNI coordinates x, y, z
IMP versus PL	115	L SMA	Area 6	5.21 (4.06)	-9, 5, 68
	98	L BCA (IFG)	Area 44	6.88 (4.62)	-57, 11, 17
		L dlPFC	Area 9	5.07 (3.98)	-54, 11, 29
	34	L lPMC (MFG)	Area 6	4.63 (3.74)	-24, -10, 53
	26	R Cb		4.77 (3.82)	30, -67, -22
IMP versus Rest[a]	107	R Rolandic	Area 4	12.84 (6.50)	63, -4, 14
		Operculum	Area 41	9.04 (5.57)	63, -10, 2
		R STG		8.96 (5.54)	51, -34, 11
	49	R STG	Area 6	8.70 (5.46)	-3, 2, 71
	34	L SMA		8.45 (5.38)	-57, -4, -4
		L STG		8.32 (5.34)	-57, -13, 2
		L STG		9.08 (5.58)	-9, -40, -40
		L Pons			
PL versus Rest[a]	51	R STG		8.40 (5.36)	54, -13, -1
		R PrCG		7.09 (4.90)	63, -4, 14
	23	L STG		8.48 (5.39)	-54, -16, 2
		L STG		6.92 (4.83)	-63, -25, 5

VI versus VP	39	L IFG	Area 45	5.62 (4.26)	-60, 11, 23
II versus IP	127	L IFG	Area 44	5.88 (4.39)	-57, 11, 17
		L MFG		4.45 (3.64)	-45, 2, 41
		L PrCG		4.29 (3.54)	-45, -1, 29
	75	R SMA	Area 6	5.18 (4.04)	12, 2, 59
		L SMA		5.03 (3.96)	-3, 5, 62
		L Cingulate Gyrus		4.51 (3.67)	-12, 5, 50
	22	L SFG		4.86 (3.87)	-24, -10, 59
VOC versus Rest[a]	62	R Rolandic Operculum		12.66 (6.46)	63, -4, 14
				9.09 (5.58)	45, -22, 8
		R STG		9.03 (5.56)	54, -13, 2
	24	R STG L STG		9.36 (5.66)	-42, -16, 35
IMG versus Rest[a]	27	R SMA	Area 6	8.22 (5.31)	3, -1, 68
		L SMA	Area 6	7.16 (4.92)	-3, -7, 71

BA, Brodmann area; BCA, Broca's area; Cb, cerebellum; dlPFC, dorsolateral prefrontal cortex; FWE, family-wise error; IFG, inferior frontal gyrus; II, imagery improvisation; IMG, overall imagery (II+IP); IMP, overall improvisation (VI+II); IP, imagery prelearned; L, left; lPMC, lateral premotor cortex; MFG, middle frontal gyrus; MNI, Montreal Neurological Institute; PL, overall prelearned (VP+IP); PoCG, postcentral gyrus; PrCG, precentral gyrus; R, right; SMA, supplementary motor area; STG, superior temporal gyrus; VI, vocalized improvisation; VOC, overall vocalization (VI+VP); VP, vocalized prelearned

Both imagery and vocalized improvisatory tasks were associated with significant changes in the lateral prefrontal cortex **(Figure 3.2)**. During overall improvisation compared to pre-learned condition, we observed widespread activations in left inferior frontal gyrus (IFG) that included the Broca's area (BCA), referred as IFG unless it is stated, dorsolateral prefrontal cortex (dlPFC), motor areas; lateral premotor cortex (lPMC) in middle frontal gyrus (MFG), referred as MFG and left supplementary motor area (SMA) plus the right cerebellum (RCb) (**Figure 3.3**). Maximum probability mapping using SPM Anatomy toolbox (http://www.fz-juelich.de/inm/inm-1/EN/Forschung/_docs/SPMAnatomyToolbox/SPMAnatomyToolbox_node.html) further confirmed the higher and significant Broca's activation in IFG during improvisation (**Figure 3.4**).

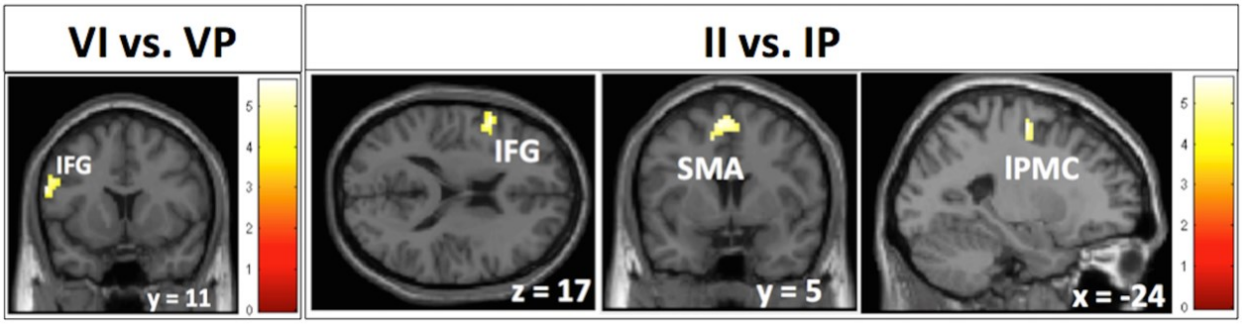

Figure 3.2 Brain Activations during vocalized and imagery improvisation

The brain activations for improvised vocalization (VI) versus pre-learned vocalization (VP) and improvised imagery (II) versus pre-learned imagery (IP)

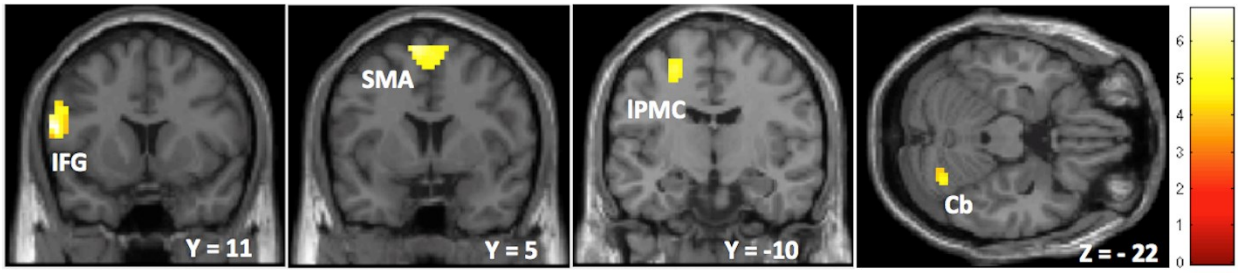

Figure 3.3 Brain Activations during overall improvisation

The brain activations for overall improvised performance (vocalized improvisation plus imagery improvisation) versus overall prelearned performance (vocalized prelearned plus imagery prelearned). The color intensity represents t-statistics, and the activations are overlaid on the Montreal Neurological Institute structural template brain in neurological orientation.

Cb, cerebellum, lPMC, lateral premotor cortex, SMA, supplementary motor area, and IFG, inferior frontal gyrus, includes both Broca's area (BCA) and dorsolateral prefrontal cortex (dlPFC)

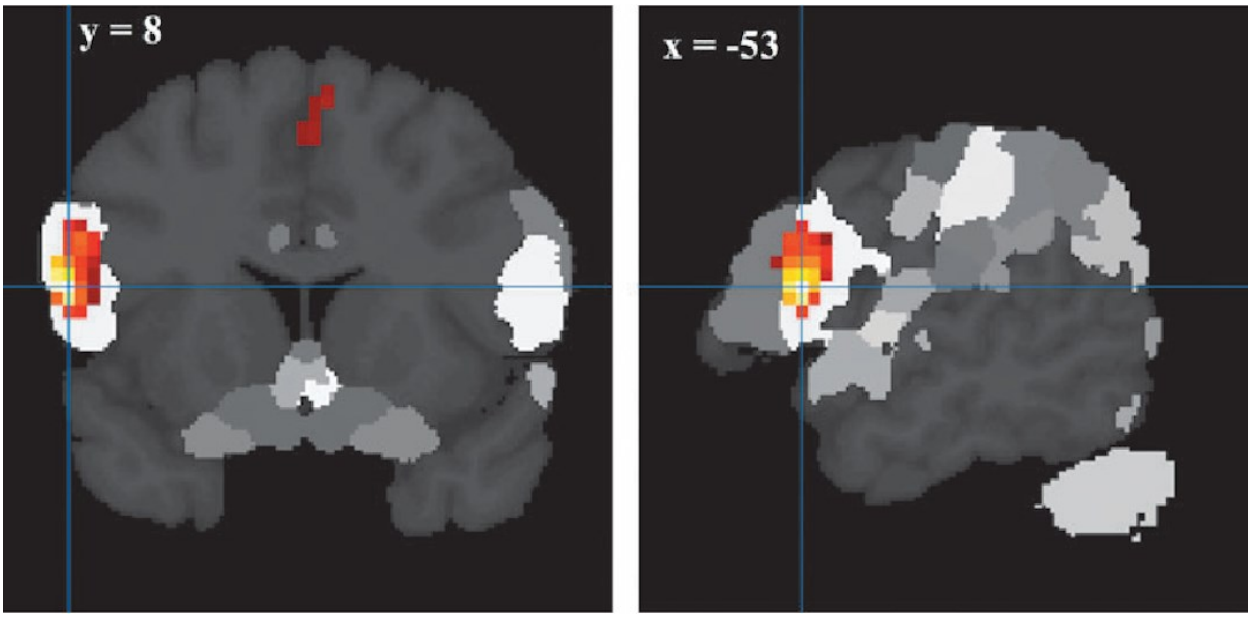

Figure 3.4 Maximum probability mapping

The overlap between the activation clusters and brain structures defined with maximum probability mapping in SPM Anatomy, the overlaid color cluster represents the functional activations on Broca's area (BCA) in the left inferior frontal gyrus (IFG) during improvisation compared to prelearned condition. Hotter the color, higher activation.

3.4.3 Network activity

We performed connectivity analysis among the six nodes: IFG, dlPFC, lPMC, SMA, RCb, and superior temporal gyrus (STG, primary auditory cortex). Inter-regional correlation analysis, as described earlier, was used to see whether these regions were functionally connected. **Figure 3.5** shows the functional connectivity during pre-learned (PL) and improvisation (IMP) condition, indicating that there was less functional connectivity during IMP compared to PL. **Figure 3.6** shows the functional connectivity during vocalize (VOC) and imagery (IMG) conditions; we found less functional connectivity during imagery compared to vocalize. Only the

functionally significant connections (significance level, $p < 0.05$) are shown in the figures with their corresponding correlation coefficient and p-values.

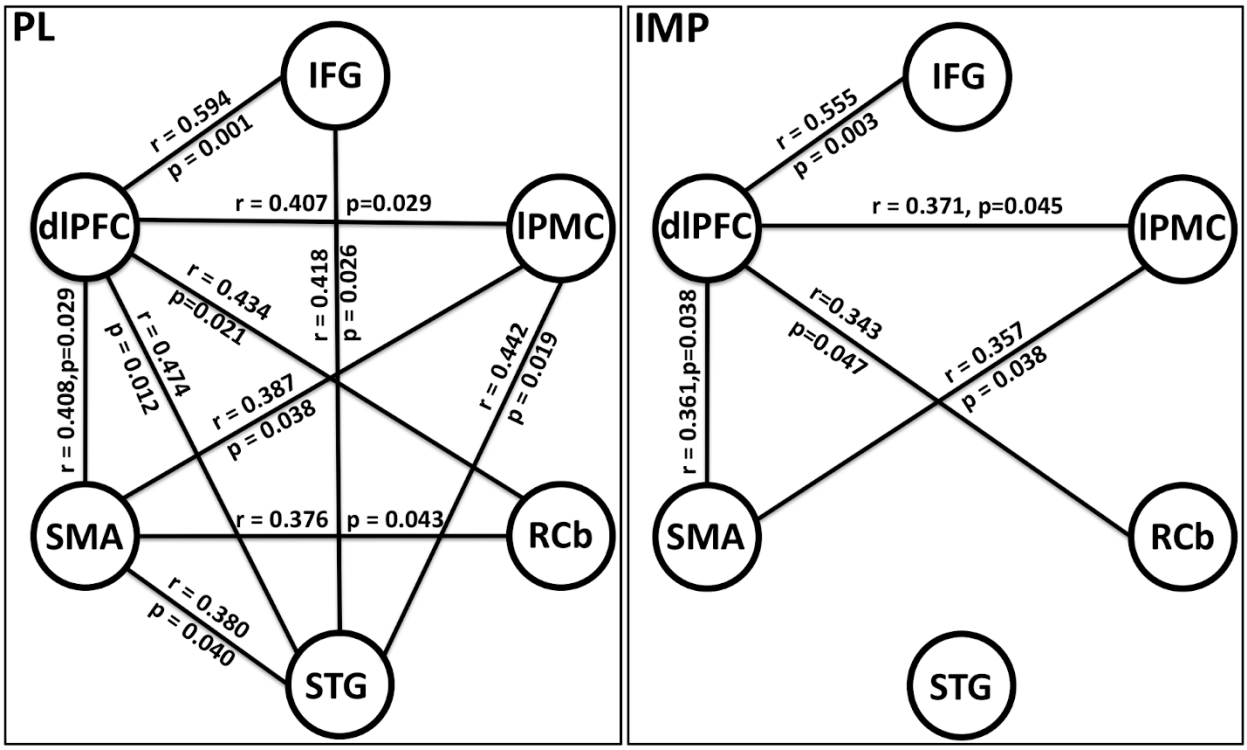

Figure 3.5 Functional connectivity during prelearned and improvised condition

Functional connectivity during overall prelearned (PL) performance (vocalize prelearned plus imagery prelearned), and overall improvised (IMP) performance (vocalized improvisation plus imagery improvisation). Only functionally significant connections ($p<0.05$) are shown here with corresponding correlation coefficient r and p-value. IFG, Broca's area at inferior frontal gurus, lPMC, lateral premotor cortex, RCb, right cerebellum, STG, primary auditory region at superior temporal gyrus, SMA, supplementary motor area, dlPFC, dorsolateral prefrontal cortex

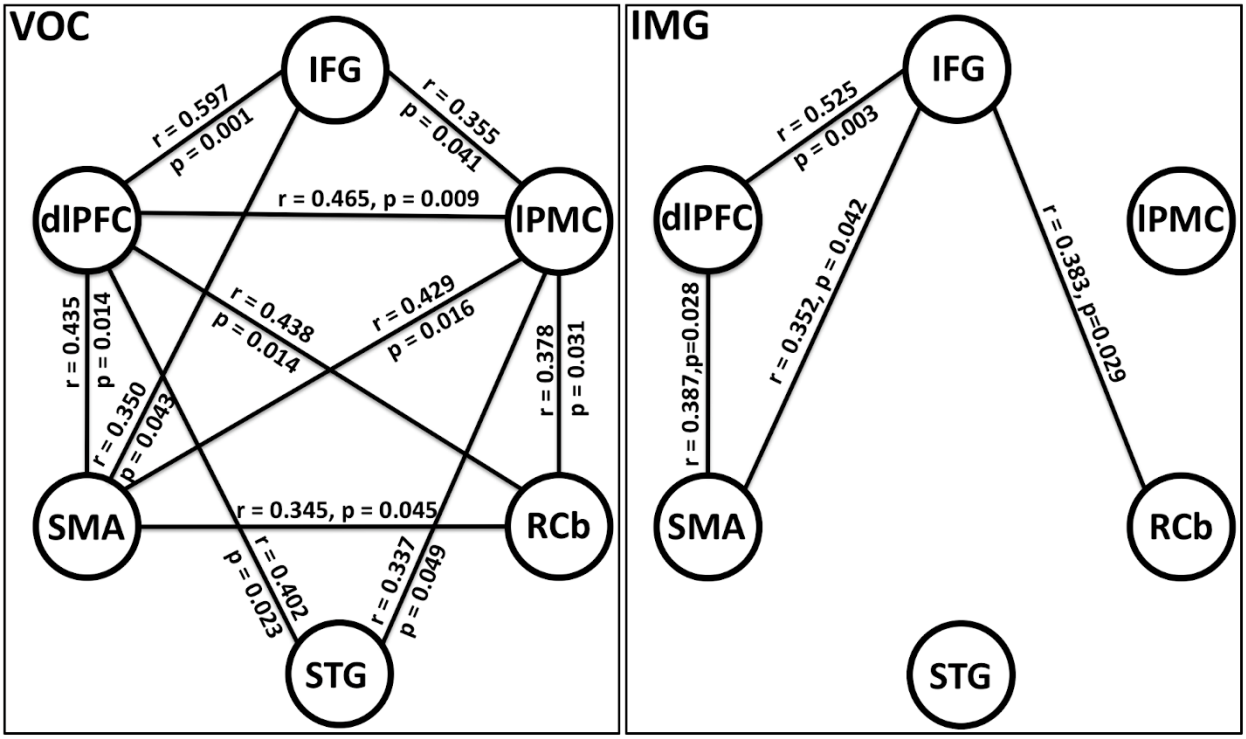

Figure 3.6 Functional connectivity during vocalized and imagery condition

Functional connectivity during overall vocalization (VOC) (prelearned vocalization plus improvised vocalization) and overall imagery (IMG = prelearned imagery+improvised imagery) task within musical improvisation and prelearned performances. Only functionally significant connections ($p < 0.05$) are shown in the figures with their corresponding correlation coefficient r and p-value.

We computed GC spectra to assess directional network interactions among the six nodes. Pairwise-GC spectra were calculated separately for the improvised and pre-learned conditions, both including vocalize and imagery conditions. We used the permutation threshold criteria to find significant causal interaction directions (details in Materials and Methods, subsection 3.3.5). The significant causal connections (schematic representation) with significant functional connections among these nodes are shown in **Figure 3.7**. **Figure 3.7** shows the significant

network interactions during PL (left panel) and IMP (right panel) conditions. The thickness of the line represents the strength of the causal interactions, as shown in each plot. The node pointed to by the arrowhead receives the causal influence from the node that line starts from. During pre-learned conditions, we found bidirectional interactions between dlPFC to all other nodes except RCb and SMA. Unidirectional causal influence was found from RCb to SMA. There were unidirectional causal influences from IFG to SMA, IFG to lPMC and IFG to RCb, which were found mediated from other nodes and hence were ruled out. We found significant unidirectional causal influence from STG to other nodes except to RCb (no functional correlation between STG and RCb, Figure 3.5). During improvisation (right panel in **Figure 3.7**), the network interactions from dlPFC to STG and SMA to RCb were ruled out as they were found to be mediated. During improvisation, we found the bidirectional interactions from dlPFC and RCb, unidirectional causal influence from dlPFC, and STG to lPMC and from lPMC to SMA.

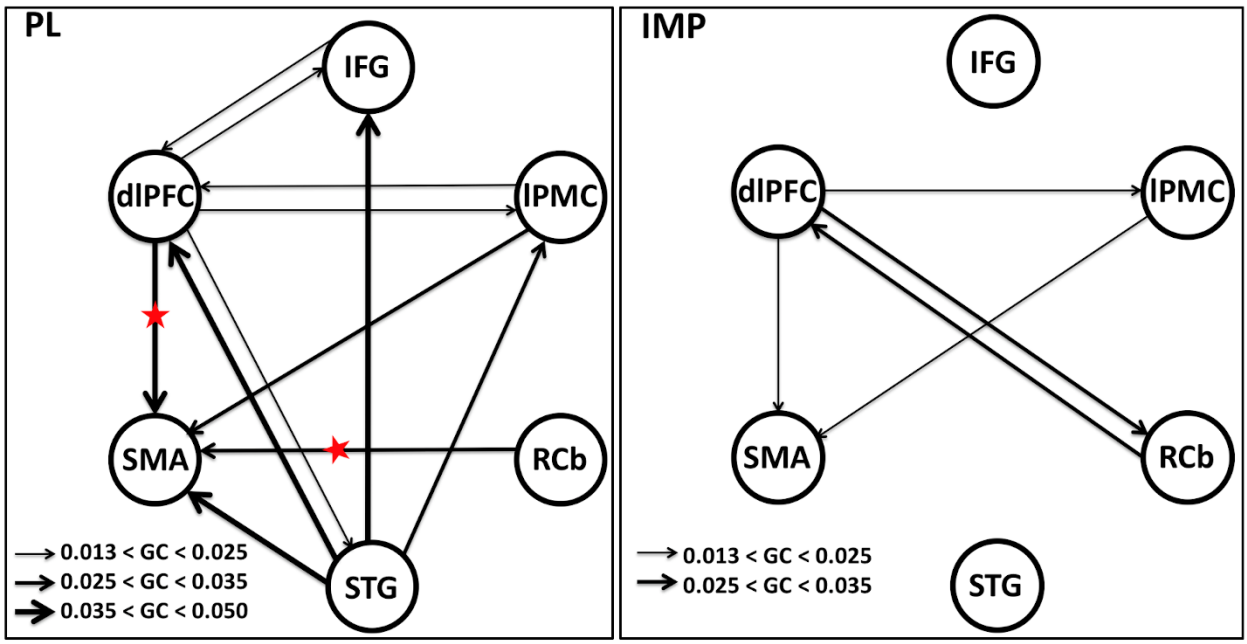

Figure 3.7 Network interaction during prelearned and improvised condition

Schematic representation of significant causal interaction directions among six nodes. The significant causal interaction for overall prelearned (PL) performance and overall improvised (IMP) performance, as determined by using permutation threshold criteria ($p<10^{-6}$), are shown by a solid line with an arrowhead; the width of the line represents the connection strengths (maximum Granger Causality values), thicker the lines more the causal strength. The red stars (left panel) represent an increase in network interaction directions ($p<0.05$) when the causal strength during overall prelearned is compared with overall improvisation.

We performed the analysis to find out how causal interactions changed during different task conditions. The time-domain GC values calculated from the entire frequency range from all the participants were compared across task conditions for statistical significance using paired t-tests. When the causal interaction strengths during pre-learned were compared to the causal interaction strengths during improvisation condition, the directed interactions from dlPFC and RCb to SMA were found significantly increased ($p<0.05$) and is indicated by a red star (**Figure 3.7**). No other interaction directions changed significantly. We also compared the causal interaction strengths between task conditions (imagine and vocalize) within musical IMP and PL. We found significant increases ($p<0.05$) in bidirectional interactions between dlPFC and SMA and unidirectional interaction from RCb to SMA during vocalize pre-learned condition compared to vocalize improvised condition, as marked by a red star (left panel, **Figure 3.8**). During imagine pre-learned compared to imagine improvised significant increases ($p<0.05$) in the directed causal interactions were found from Broca's area (IFG) to RCb and SMA, and dlPFC to SMA as marked by a red star (right panel, **Figure 3.8**). We showed only the directions, which

are functionally connected with task conditions, and causal interactions are significant, ruling out the mediated interaction from the conditional GC analysis.

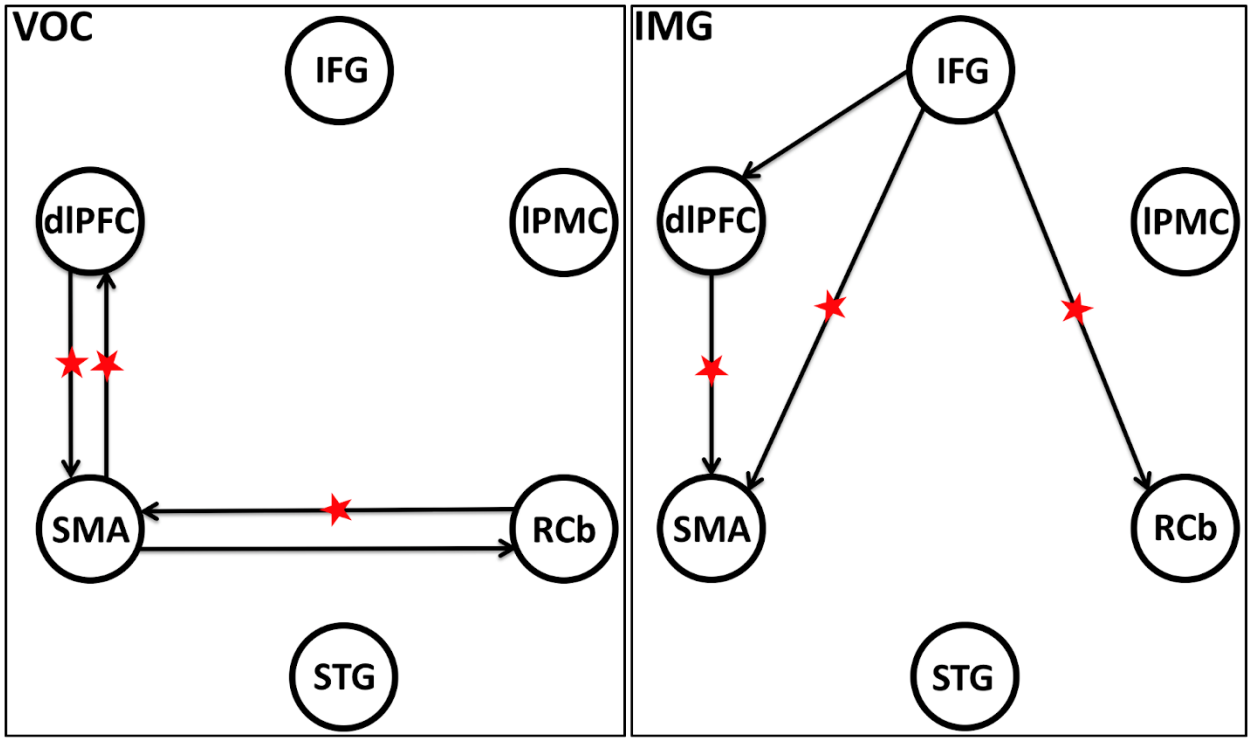

Figure 3.8 Network interaction during vocalized and imagery condition

Network interaction modulation. Significant changes in network interactions ($p<0.05$) are marked with a red star during vocalized prelearned compared with vocalized improvisation in the left panel (VOC), and imagery prelearned compared with imagery improvised in the right panel (IMG). A red star represents the increase in network interaction.

3.5 Discussion

Here we investigated fMRI BOLD responses during vocalized or imagined musical performance of melodies retrieved from memory (pre-learned condition) followed by improvisations (improvised condition) on the same chordal structure. In the current paradigm improvised and pre-learned conditions, both gave rise to similar motor actions, only the mode of

creation was different. The neural correlates behind this difference were the focus of the current research. We found that musical improvisation is characterized by significant changes in frontal cortices, increased widespread activity in the left IFG including Broca's area (BCA), dlPFC, and extended to the motor areas lPMC in the middle frontal gyrus (MFG), SMA and RCb (**Figures 3.2, 3.3 and 3.4**). Interestingly, the functional connectivity, as measured by correlations, was significantly less during improvisation (**Figure 3.5**). The causal interaction strengths during pre-learned conditions from dlPFC and RCb to SMA were significantly increased compared to the improvisation (**Figure 3.7**). Furthermore, we found the significant increase in the directed causal interactions from dlPFC and RCb to SMA (left panel, **Figure 3.8**) during vocalize pre-learned compared to vocalize improvised, and from IFG to RCb and SMA, and dlPFC to SMA (right panel, **Figure 3.8**) during imagine pre-learned compared to imagine improvised. Below we discuss why improvisation leads to increased node activation but decreased connectivity from higher-level prefrontal control to motor planning areas.

Cognitive processes underpinning musical improvisation include fitting responses to an overall architectural structure, combining discrete chunks into an action chain, and selecting individual auditory and motor chunks [45, 64]. The activation of BCA during improvisation in the current study may indicate the central role of BCA in the generation, and selection, and execution of action sequences. Specifically, BCA has been implicated in higher-order chunking mechanisms that are central to hierarchically organized sequences [51]. Tonal music is hierarchically organized both according to tonal and rhythmic hierarchies [49], and tonal jazz improvisations show statistical distributions similar to other tonal music [86]. Therefore, BCA may control the selection and concatenation of auditory chunks that together form a syntactically pleasing sequence that displays these hierarchies [47]. However, this interpretation of the

activation does not explain why connectivity during improvisation (IMP) is less than during pre-learned (PL) performance. The regional brain (node) BOLD response can be attributed to: the synaptic input to the neuronal population of that region and its intrinsic processing [11, 12]. The intrinsic processing dominantly contributes to the overall activity (up to approximately 79%) [87]. Consistent with these findings, it is reasonable to assume that the elevated activity in IMP compared to PL is most likely to be related to the additional cognitive load fulfilled by intrinsic neural processing in each brain area rather than greater coordination among areas as in PL. We offer two explanations for this observed phenomenon; one related to Broca's involvement in evaluation processes and another related to the translation of abstract information to motor commands.

It is possible the higher node activity in the cognitive control areas is related to ongoing evaluation of ideas [48] but that most of those ideas were initially appropriately alleviating the need to communicate corrective information to the motor areas. New research investigating the role of IFG in a traditional alternative uses creativity task indeed found that left IFG is specifically involved in the evaluation of creative ideas after they have been generated by neural structures associated with the default mode network [88]. During musical improvisation, the real-time demands of the task most likely involve continuous generation with concurrent evaluation [89]. This is in opposition to traditional creative tasks like poetry generation [90] and painting [91], in which the lack of time constraints allow for the separate generation and evaluation stages. In the current study, we postulate that the subjects, who were advanced improvisers with extended knowledge of the dictated harmonic context, the bottom-up generative processes served up mostly appropriate ideas [61]. Though frontal cortical regions monitored the output more closely during improvisation due to the novelty of the generated responses (higher activation),

the initial ideas were mostly appropriate. Therefore, the output of the executive network evaluation did not need to be communicated to motor regions (less connectivity). On the other hand, during the pre-learned condition, an exact auditory picture retrieved from memory was constantly being compared to the actual output and detailed adjustments communicated continuously from executive control areas to motor planning regions resulting in higher connectivity. However, since no retrieval and concatenation of novel output was required, activation of the ECN areas was less than in the improvisation condition.

It has recently been suggested that musical improvisation, as well as other creative behaviors, rely on a constructive interplay between the DMN and ECN [46]. Indeed, the activation of control areas and the coupling of the ECN and the DMN appears to be directly related to the amount of goal-directed processing necessary for the task. Pinho et al. (2016) compared two types of improvisation tasks and found a network similar to the network identified in the current study (frontal-motor) during a task in which participants were required to use a specific pitch set during improvisation. They identified a different network (frontal to DMN) in a task in which improvisers were simply required to communicate emotions. In the current study, we compared network activity between specified nodes as opposed to Pinho et al. (2016) [64], who used a seed region to identity two different networks. In addition, we used the pre-learned/improvised contrast, whereas Pinho compared two types of improvisation. Nonetheless, it is interesting that their pitch set condition pointed to a network where dlPFC was connected to motor regions similar to the network we identified. However, we found less connectivity in this network during improvisation compared to pre-learned. It may be that the highly-constrained pitch set improvisation condition in some ways was more similar to our pre-learned condition.

Future research could evaluate the effect of constraints and goal-directedness on top-down control and related connectivity during improvisation (Beaty, 2016)[46].

Another possible explanation for the observed node activation accompanied by attenuated connectivity may be related to the role of IFG in translating abstract information to motor commands. This process has been described in another domain that is associated with the production of hierarchically organized structures: language [92]. The traditional role of BCA as related to speech production has recently been investigated further [93]. It appears the area is engaged in mediating the interaction between temporal and frontal regions by translating abstract information into articulatory code. However, as this code is implemented by the motor cortex, BCA is surprisingly silent [93]. In the current study, this same translation of the auditory image of the retrieved longer pre-learned melodies into motor commands may account for the increased connectivity during the pre-learned condition. Even during imagery, the motor planning areas are known to be active, presumably requiring a translation process [94]. Yet, as above, no concatenation of novel output following syntactic rules was required in this condition as the pre-learned melodies are retrieved in a fully intact form (less node activation). We postulate that the translation of auditory image to motor commands is needed less during improvisation because auditory chunks offered up by the default network are already linked to their related motor commands (less connectivity). Yet, BCA is still engaged in concatenation of these chunks (more node activation). Future research could investigate this idea by manipulating the links between auditory image and motor commands of chunks used during improvisation. This could be done in an instrumental improvisation task by changing the key in which improvisations are performed from a familiar key where auditory image and motor commands are linked to an unfamiliar key [95].

The areas that exhibited increased activation during improvisation in the current study were dlPFC, lPMC, SMA, and RCb. The dlPFC is also associated with goal-directed behaviors that are consciously monitored, evaluated, and corrected as described above and is a central part of the ECN. Specifically, dlPFC may be involved in inhibiting habitual responses [63]. Thus, the activation of left dlPFC during improvisation may indicate top-down control, attentional monitoring, and evaluation, which are consistent with previous studies and consistent with functions of the ECN [47, 60]. The activation of the motor planning areas, lPMC in MFG, and SMA during improvisation may be due to the process of selecting single motor acts or single sensorimotor associations associated with the hierarchical organization of the human behaviors [50]. These areas have also been implicated in previous research involving various music improvisation tasks [47]. Finally, the Cb may be associated with movement coordination and maintenance of an internal pulse [96, 97]. Cerebellar activation has specifically been observed when subjects move to both heard and imagined music [98]

In the current study, we did not find differential activations in medial prefrontal and parietal regions in the pre-learned versus improvisation contrasts [61]. We, therefore, did not find a specific support for the activation of the DMN during improvisation [64]. This difference, compared to previous findings, is most likely due to the current paradigm using vocalization and imagery. Future studies using the current paradigm with a larger sample size should investigate both the role of the ECN evidenced in the current study and the complementary contribution of the DMN. Furthermore, future studies should investigate the role of expertise using the current paradigm. The current sample only included experts, and the available audio recordings of improvisations were all judged highly accurate, reflecting both adherence to the underlying harmonic progression and rhythmic pulse. The little discrepancy during performances does not

reflect in cluster level activation in the brain during vocalized improvisation, and the details are discussed in **Appendix (A.1)**. We had audio from only 13 subjects to analyze, and an obvious limitation of the current paradigm is the lack of ratings for the imagined trials where only overall timing could be used for trial validation. The strength of this study compared to the previous studies is that the potential confounds of the overt movement were avoided in musical improvisation. Although the brain activations result of contrasting the vocalize-condition with the imagine-condition or vice-versa are not considered in the result section, we have looked at these contrasts, and the details are discussed in **Appendix (A.2)**.

3.6 Conclusion

In conclusion, we found differences in activation and connectivity between the closely matched performance of prelearned and improvised melodies. To our knowledge, this is the first study to investigate this contrast using vocalization and imagery tasks. The observed node activations during improvisation appear to confirm the central role of Broca's area in the creation of novel musical output. Yet, the accompanying attenuation of connectivity supports the idea of limited top-down control. It is possible that this apparent disassociation between node activity and functional connectivity is central to the cognitive underpinnings of real-time creativity.

4 WHITE MATTER FIBER TRACTS AND STRUCTURAL NETWORK

4.1 Introduction

Human cognition and behavior arise from neuronal interactions over brain-structural networks. These neuronal interactions cause changes in structural networks over time. How a creative activity such as musical improvisation performance changes the brain structure is largely

unknown. Examining the brain circuitry for creativity by using advanced brain imaging techniques has been an active field of research in recent years in efforts to understand the neural underpinnings of human creativity. Musical improvisation being one of the most complex forms of creative behavior, has been used to understand real-time creativity, where revision is not possible. As reviewed in contemporary literature [3, 46, 99], variations in brain activity and connectivity refer to the heterogeneity of the participant's background, their learned skills, experience, and creative expertise. In a recent neuroimaging study of advanced jazz musicians, we explored the divergent brain activation and connectivity patterns during musical improvisation and non-improvisation tasks. This functional magnetic resonance imaging (fMRI) study revealed higher regional activity in the inferior frontal gyrus (IFG), including the dorsolateral prefrontal cortex (dlPFC) and Broca's area (BCA), lateral premotor cortex (lPMC), supplementary motor area (SMA) and cerebellum (Cb), with less functional connectivity in number and strength during musical improvisation compared with pre-learned melody [100]. The directed functional connectivity further revealed that dominant information flow is from the lateral prefrontal cortex to the supplementary motor area in both conditions. The central roles of BCA, dlPFC, lPMC, and SMA have been widely discussed in creativity, both in domain-specific and domain-general abilities [3]. Although the studies have reported the consistent recruitment of the lateral prefrontal cortex and SMA in creative tasks, the network interaction patterns are varying across studies. During musical improvisation, the real-time demands of the task most likely involve continuous generation with concurrent evaluation [89]. Acquired skills, training, experience, and knowledge, enable advanced improvisers to produce spontaneous performances, automatically controlling the interplay between perception, attention, and memory. This may result in an attenuated network interaction during improvisation, a state that has been referred to

as hypofrontality [101]. These processes could result in the observed pattern of increased node activation and decreased connectivity during improvisation [100].

It is largely unknown how such divergent activity and connectivity patterns in experts emerge from the underlying brain structural organization and fiber architecture. While considering the dynamic functional states of activity and connectivity during creative performances, it is important to consider the behavioral consequences in the microscopic structural organization as well, particularly in white matter fiber properties. To characterize the brain structure, studies have investigated the variation in grey matter and white matter properties, associated with expert populations related to their cognitive skills, training/practice, experience, creativity, and behavioral expertise [102-106]. Despite the growing evidence of structural brain differences between musicians and nonmusicians, whether and how the underlying white matter fiber properties reflect the neural activity and network interaction is not clearly understood. Comparing musicians with nonmusicians, significant differences have been found in the corpus callosum, arcuate fasciculus, internal capsule, corticospinal tracts, superior longitudinal fasciculus, superior temporal gyrus, cerebellar peduncle, inferior-fronto-occipital fasciculus, uncinate fasciculus, inferior longitudinal fasciculus and fiber tracts connecting posterior superior temporal gyrus and middle temporal gyrus [102].

Previous studies have mainly investigated structural pathways and direct fiber trajectories in terms of fractional anisotropy (FA), using diffusion tensor imaging (DTI), a method that relies on the movement of water molecules (i.e., how fast water molecules move along axonal fiber tracts) [14, 15]. Variations in FA in white matter microstructure have been reported at both the individual and group levels [107, 108]. But inconsistency in findings across studies might be due to types of musician studied, including whether trainee or advanced level, skills, experience &

expertise, improvisers or non-improvisers in addition to the properties measured and analysis methods. FA provided from the DTI method is an ensemble measurement and suffers from a partial volume effect, which may lead to inaccurate anisotropic measurement in complex fiber structures such as crossing fibers, free water diffusion in ventricles, and non-diffusive particles [44]. Here, we study the brain structural differences between advanced jazz improvisers and nonmusicians (control group). We examined the white matter diffusion properties in terms of quantitative anisotropy (QA), using the Q-Space diffeomorphic reconstruction (QSDR) approach [27, 44] implemented in DSI studio toolbox (http://dsi-studio.labsolver.org/). The QA measure used in this study is different than the traditionally used fractional anisotropy (FA). The measurement of QA is based on the model-free nonparametric approach, which calculates the density distribution of water diffusion. QA is calculated from the peak orientations on a spin distribution function and is reported to have lower susceptibility to partial volume effects of crossing fibers and free-water, resulting in a better resolution with QA-aided tractography, which is known to outperform the FA-aided tractography [28, 44]. Since QA is sensitive to the compactness of the fiber bundle, the normalization of QA (NQA) reduces the variability resulting in a stabilized spin-density measurement across subjects. In addition to NQA measures, we have examined the generalized fractional anisotropy (GFA), whose calculation is also based on the orientation distribution function [24] and has a high correlation with FA [109].

The regional and track-specific analysis is based on the functional network reported in our previous fMRI study of the same advanced jazz improvisers [100]. The regional analysis includes brain areas dlPFC in IFG, lPMC in MFG, SMA, cerebellum (RCb), and superior temporal gyrus (STG), whereas the track-specific connectivity analysis includes the fiber pathways connecting those brain areas. The regional and track-specific fiber architecture were

investigated using the QSDR approach to test whether there were any significant differences in their underlying white matter diffusion properties and how this structural architecture varied from the control group of nonmusicians. We compared both the track-specific and regional NQA measures of advanced jazz improvisers with a control group of nonmusicians. Secondly, we compared the regional and track-specific anisotropy measures of advanced jazz improvisers with their brain activity and connectivity pattern, to assess the consistency of the white matter fiber integrity and the brain functional states, especially the lateral prefrontal and supplementary motor areas and network interaction between those areas.

4.2 Materials and Methods

4.2.1 Participants

We studied two groups of healthy adults, matched as closely as possible in gender, age, and handedness. The "improvisation" group consisted of 20 advanced jazz improvisers (mean age ± standard deviation (sd)=30.9±13.3 years). For jazz-improviser, a criterion for participation was expertise in jazz improvisation. Jazz improvisers had at least six years of professional experience (mean ± sd=20.2±12.8 years) on jazz improvisation (see **Table 3.1**). Almost all the jazz improvisers had previous education in a University System School of Music; average schooling years for all participants was 16.2 years (sd=1.8 years). Improvisors were also required to know how to read music. Primary instruments included piano (n=5), saxophone (n=9), guitar (n=1), trumpet (n=2), drums (n=1), trombone (n=1) and bass (n=1). The "control" group consisted of 20 nonmusicians (mean age ± standard deviation (sd)=29.4±4.4 years) who never past childhood played a musical instrument and had no previous music education.

All participants had normal or corrected to normal vision and reported normal

neurological history. Participants provided written and signed consent forms and were compensated for their participation in the experiment. Institutional Review Board for Joint Georgia State University and Georgia Institute of Technology Center for Advanced Brain Imaging, Atlanta, Georgia, approved this study.

4.2.2 Behavioral tests and MRI scanning

Upon arrival at the testing site, participants provided informed consent and were familiarized with brain imaging methods. They went through practice sessions at a mock scanner to reduce anxiety and make sure they are comfortable about the MRI before going into the scanner for actual diffusion weighted imaging (DWI). They were asked to remain still, not to move their head or other parts of their body during the recording. Foam pads were used as support in the head coil to constrain head motion.

4.2.3 Data Acquisition and Preprocessing

Diffusion-weighted imaging (DWI) data were acquired along 60 sampling directions. The b-value was 1000 s/mm$^{2.}$ The b-value is a factor that measures the degree (strength and timing) of the diffusion weighting applied. The slice thickness was 2mm. A pair of images with no diffusion weighting (b0 images) was also acquired. We converted DWI data from DICOM to NIFTI format by using the dicom to nii (dcm2nii) toolbox part of the MRIcron. During this step, a *b*-value and *b*-vector file were generated along with the standard NIFTI file. Next, we performed standard eddy current correction using the FMRIB Software Library v6.0 processing software package (https://fsl.fmrib.ox.ac.uk/fsl/fslwiki/FDT/UserGuide) on DWI data for head motion and eddy correction. Next, we imported DWI data in DSI-Studio (http://dsi-studio.labsolver.org/) and examined by a quality control procedure to ensure its integrity and quality [110]

4.3 Data Analysis

4.3.1 Behavioral data analysis

Behavioral data for advanced jazz improvisers were recorded on the computer that also ran the E-prime program displaying the experimental task sequences. The audio output (vocalized melodies and improvisations) was recorded as MP3 files using an fMRI scanner compatible microphone. Stimulus onset time and the time between the onset of a condition and the button press (start of improvisation) in each trial were recorded. Audio files were analyzed to determine participants' performance accuracy in reproducing the cued melodies. The improvisations were evaluated to ensure they implied the dictated blues chord progression. Any performed trials or runs with inappropriate duration (taking a long- or short-time duration) were dropped and thus not included in data analysis. Behavioral data analysis were already discussed in the previous chapter, see details in subsections 3.3.1 and 3.4.1.

4.3.2 Diffusion weighted imaging data analysis

For each participant, we estimated the anisotropic diffusion parameters mean GFA and mean NQA, using the Q-space diffeomorphic reconstruction (QSDR) approach [28, 44] implemented in DSI Studio (http://dsi-studio.labsolver.org). QSDR is a model-free generalized Q-sampling imaging (GQI) approach, which calculates the density distribution of water diffusion at different orientations using a high- resolution standard brain atlas constructed from 90-diffusion spectrum imaging datasets in the ICBM-152 space. In QSDR, DSI Studio first calculates the quantitative anisotropy (QA) mapping in the native space and then normalizes it to the MNI QA map. We performed Quality Check to make sure the "Neighboring DWI correlation," the R-squared values between the subject QA and MNI QA map, were significant

enough. The lowest “Neighboring DWI correlation” value was 0.8, which is significantly higher than the suggested R-squared value of 0.6.

A whole brain tractography was performed. A deterministic fiber tracking algorithm [27, 28, 44] was used. The QA threshold was 0.12. The angular threshold was randomly selected from 15 degrees to 90 degrees. The step size was chosen randomly from 0.5 voxels to 1.5 voxels. The fiber trajectories were smoothed by averaging the propagation direction with a percentage of the previous direction. The percentage was randomly selected from 0% to 95%. Tracks with a length shorter than 30 or longer than 200 mm were discarded. A total of 100000 tracts were calculated. We applied Topology-Informed Pruning (TIP), which increases the accuracy by using the topology of a tractogram itself to identify the candidate of false connections for removal [111]. For each participant, GFA and NQA were estimated for all the possible tracts crossing five brain areas, namely the dlPFC, the lPMC, the STG, the RCb, and the SMA and the fiber pathways connecting these areas. The dlPFC in this study refers to a combined cluster of Brodmann area 9 (dlPFC) and 44 (Broca's area) in the left inferior frontal gyrus (IFG) identified in our fMRI study [100]. To ensure consistency across subjects, we normalized the QA measure by scaling the subject-wise maximum QA value to 1. Normalization of QA assumes that all the subjects have the same compactness of white matter. To avoid any bias among participants, an identical set of tracking parameters was used for jazz improvisers and control nonmusicians.

4.4 Results

4.4.1 Behavioral results

The behavioral data were analyzed to make sure the task performances of the advanced jazz improvisers. Any trial or run with inappropriate performance duration, either too long or too

short duration, was not included in the data analysis. Trials were monitored during data acquisition and compared with the expected length. Four participants (participant numbers 7, 11, 20, and 23, shown in bold italic faces in **Table 3.1**) had all runs with inappropriate performance duration and were excluded from fMRI data analysis and thus are also excluded here in diffusion weighted imaging data analysis. Excluding those four improvisers resulted in a mean age – SD and mean years of experience – SD of 30.9 – 13.3 years and 20.2 – 12.8 years, respectively. The "control" group consisted of 20 nonmusicians (mean age ± standard deviation (sd)=29.4±4.4 years) who rarely played a musical instrument and had no previous music education. Behavior results for advanced jazz improvisers are already discussed in the previous chapter; see details in subsection 3.4.1.

4.4.2 White matter fiber tracts results

To determine diffusion parameters, we first performed whole-brain tractography, followed by limiting the white matter tracts to those passing through the 5 predefined seed regions, namely—the dlPFC, the lPMC, the STG, the RCb, and the SMA, and explored the fiber pathways connecting these regions. The selection was based on our previous fMRI study of the same advanced jazz improvisers, where these five regions showed higher brain activations during improvisation compared to pre-learned [100]. In **Figure 4.1,** we show fiber tracts crossing through seed region dlPFC, and in **Figure 4.2,** we show the underlying fiber pathways between dlPFC and SMA for a representative participant. Here, fibers are colored-coded to represent their orientation, where "red" indicates fibers along the *X*-axis (i.e., left-right), "green" indicates fibers along the *Y*-axis (i.e., anterior-posterior), and "blue" indicates fibers along the *Z*-axis (i.e., inferior–superior).

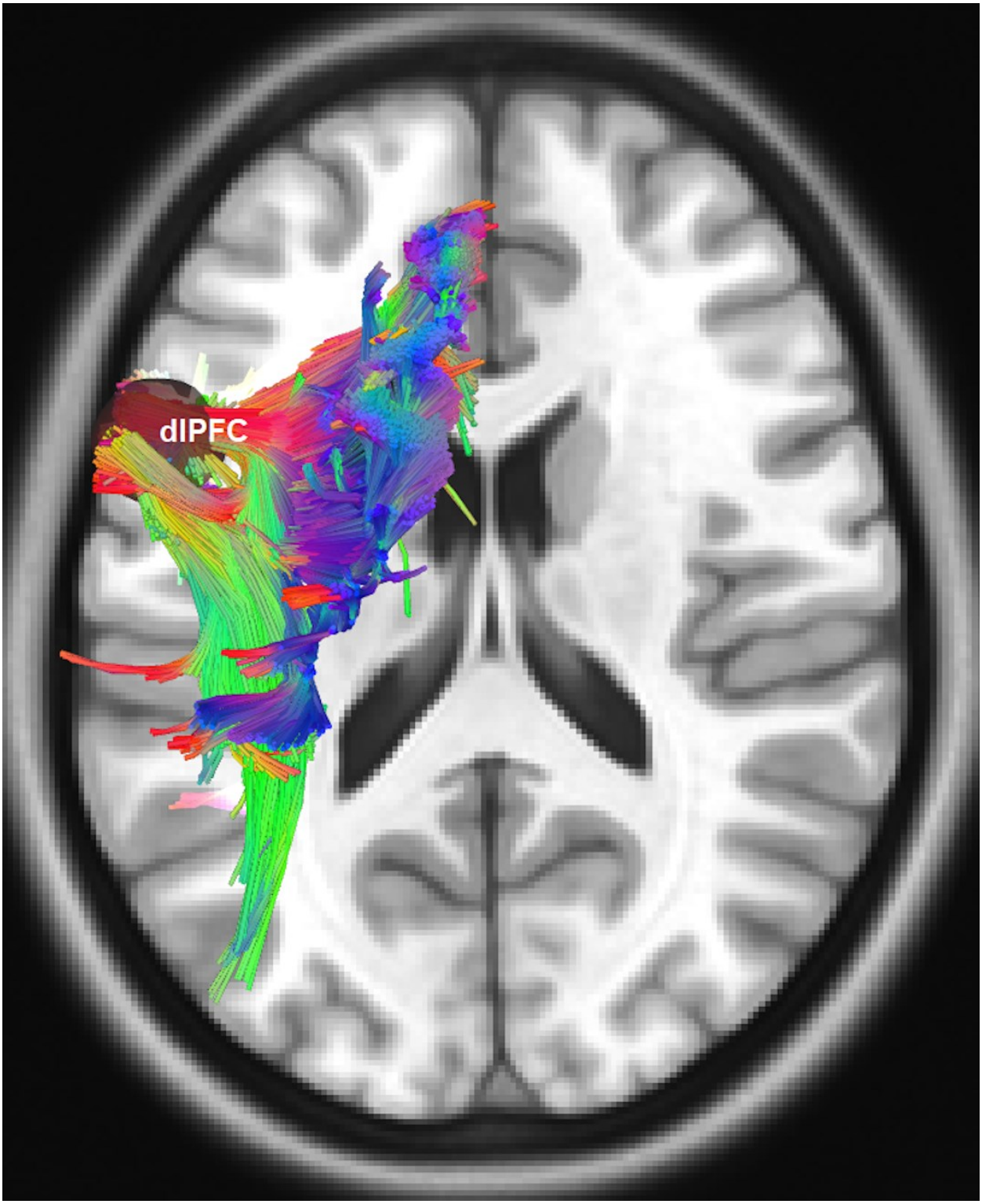

Figure 4.1 Region-based white matter fiber tracts

Fiber tracts crossing through seed region dlPFC left dorsolateral prefrontal cortex for a representative participant. Tracts shown in red indicate a fiber direction from left to right or vice versa. Blue indicates a fiber direction from anterior to posterior or vice versa. Green indicates a fiber direction from superior to inferior or vice versa.

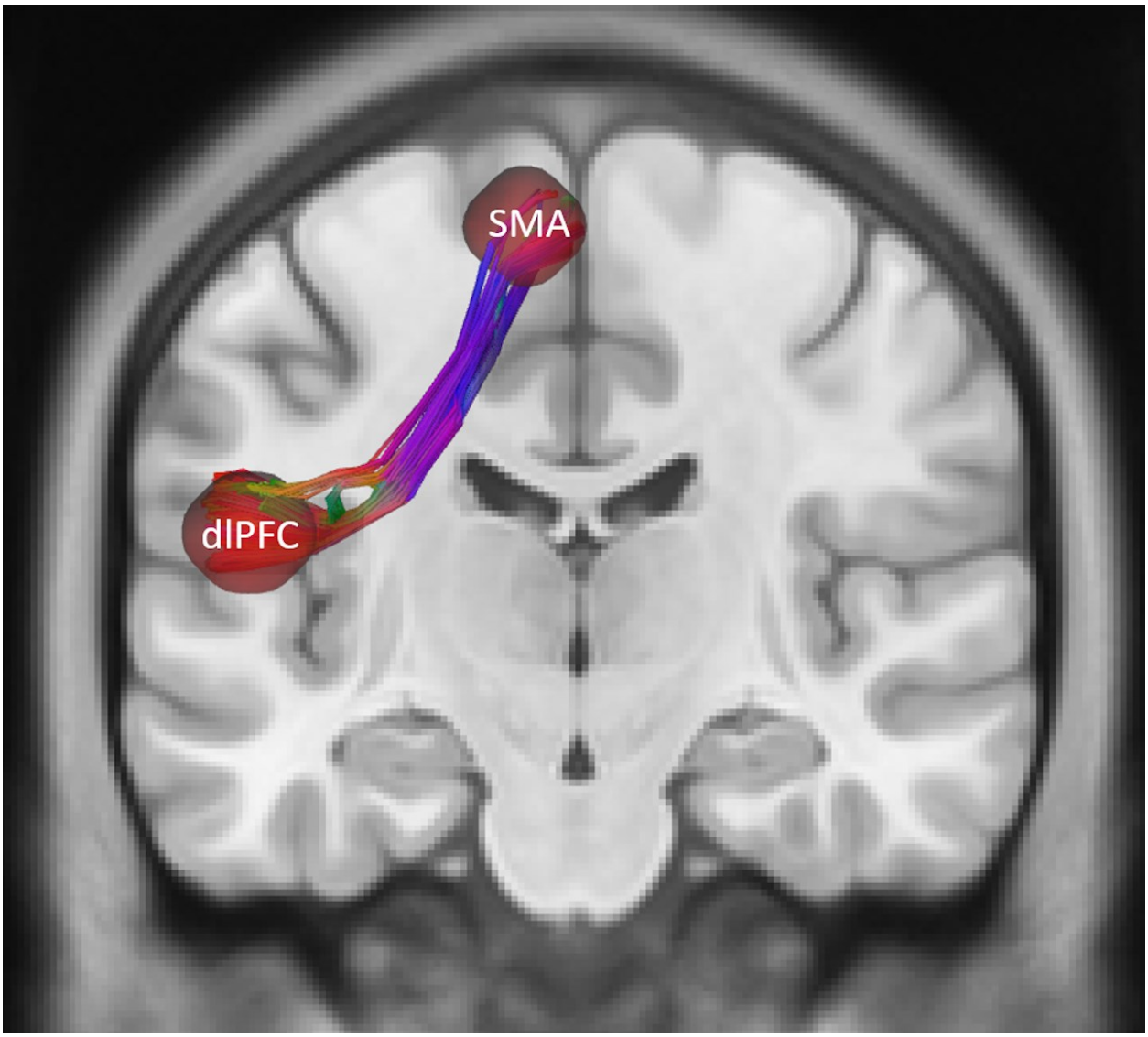

Figure 4.2 Track-specific white matter fiber tracts

Fiber pathway connecting dlPFC and SMA for a representative participant. Tracts shown in red indicate a fiber direction from left to right or vice versa. Blue indicates a fiber direction from

anterior to posterior or vice versa. Green indicates a fiber direction from superior to inferior or vice versa. dlPFC, dorsolateral prefrontal cortex, SMA, supplementary motor area

A detailed comparison of diffusion parameters GFA and NQA was performed on fibers crossing through the five specified seed regions and the underlying fiber pathways connecting them. In **Figure 4.3 and Figure 4.4**, we show the regional and track-specific NQA for advanced jazz improvisers and control nonmusicians. Advanced jazz improvisers showed significantly higher NQA measures in lateral prefrontal and motor areas (dlPFC & lPMC) and the fiber pathways connecting dlPFC to motor areas (dlPFC-lPMC & dlPFC-SMA), whereas the GFA difference between advanced jazz improvisers and nonmusicians was not significant. In **Figure A.1.2** and **Figure A.1.3** in the Appendix, we also show regional and track-specific GFA for advanced jazz improvisers and nonmusicians. Further, we checked the consistency of the functional interaction pattern of information flow from dlPFC to SMA during task performances, as observed in our previous fMRI study [100], with the underlying fiber pathways connecting dlPFC and SMA. The dlPFC-SMA fiber pathway in advanced improvisers is enhanced with higher NQA measures compared to nonmusicians. In **Figure 4.5,** we show the result of overall dlPFC-SMA directional connectivity, as revealed by the Granger Causality (GC) analysis method using our functional MRI data. Similar connectivity results were reported in our previous fMRI study [100]. The left panel (A) represents the information flow from dlPFC to SMA during pre-learned (PL) and improvised (IMP) conditions, whereas the right panel (B) represents the enhanced fiber pathway connecting dlPFC and SMA in advanced jazz improvisers. Interestingly, the connectivity is higher the pre-learned condition compared to improvisation between these two areas.

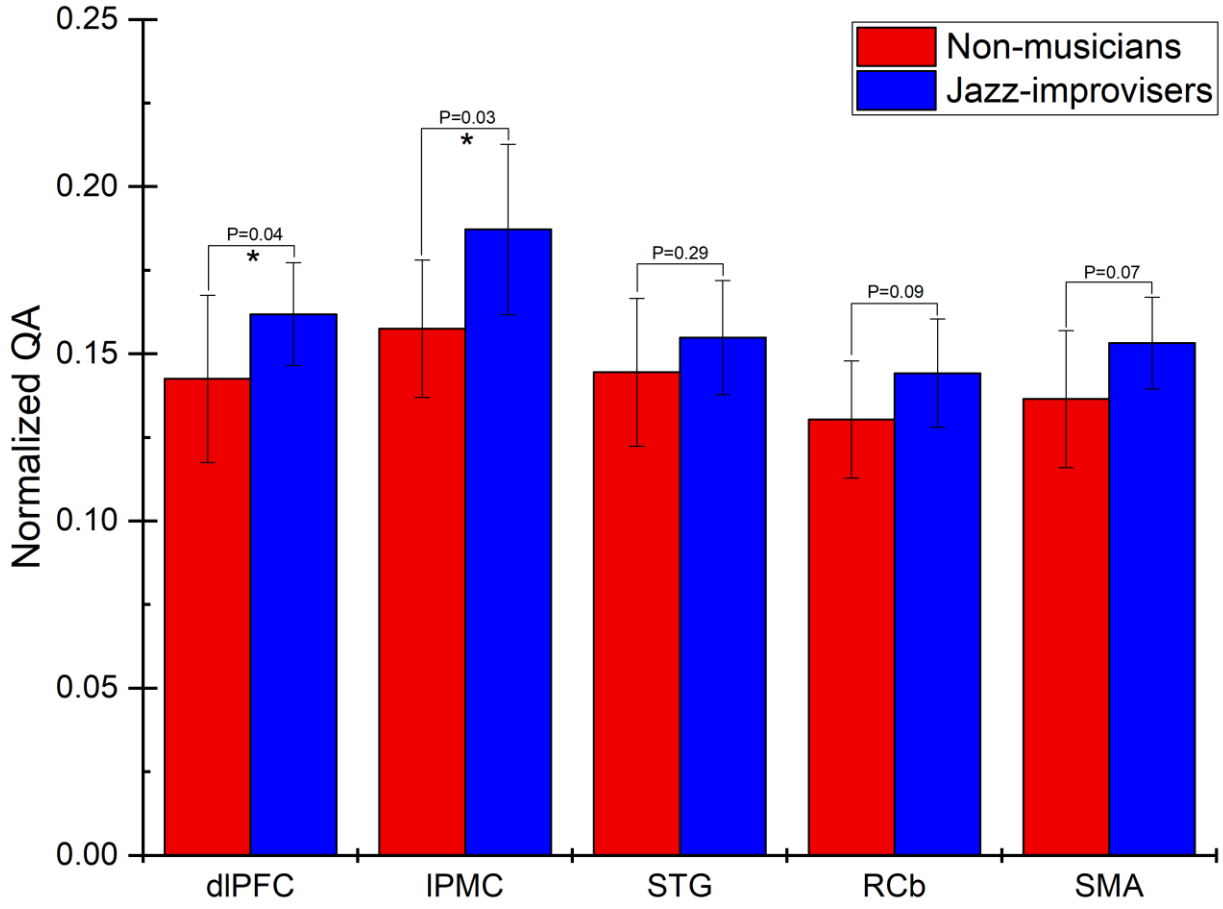

Figure 4.3 Region-based normalized quantitative anisotropy

Region-based normalized quantitative anisotropy (NQA) for advanced jazz improvisers and control nonmusicians. Compared to nonmusicians, advanced jazz improvisers have significantly higher NQA measures in lateral prefrontal regions (dlPFC & lPMC)

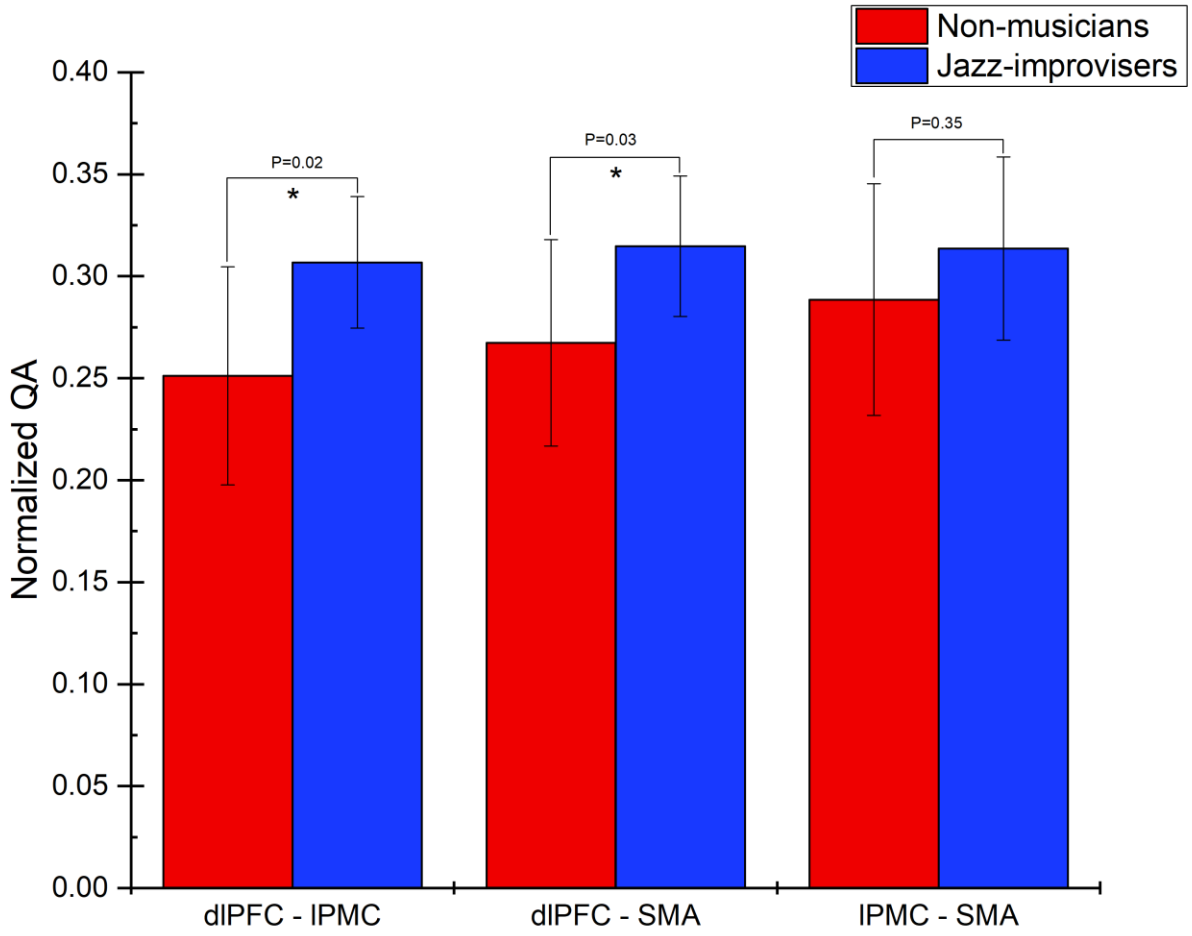

Figure 4.4 Track-specific normalized quantitative anisotropy

Track-specific normalized quantitive anisotropy for advanced jazz improvisers and control nonmusicians. Compared to nonmusicians, advanced jazz improvisers have significantly higher NQA measures in the fiber pathways connecting lateral prefrontal (dlPFC) and motor areas (lPMC & SMA)

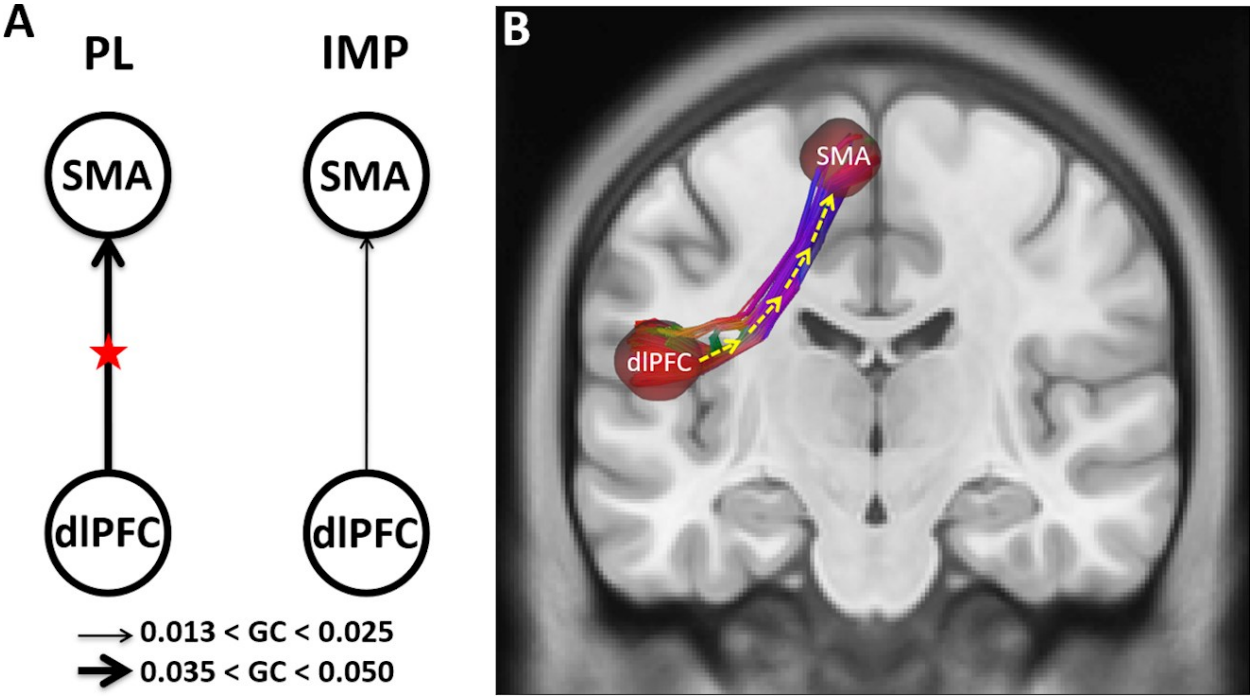

Figure 4.5 Functional and structural network

Schematic representation of significant causal interaction directions and structural connectivity between the dorsolateral prefrontal cortex (dlPFC) and supplementary motor area (SMA). (A) Causal flow from dlPFC to SMA during prelearned and improvisation conditions. The red stars (left panel) represent an increase in network interaction directions ($p<0.05$) when the causal strength during overall prelearned is compared with overall improvisation. (B) Underlying white matter fiber pathway connecting dlPFC and SMA. Overlaid arrowhead represents the corresponding causal directionality in the functional network

4.5 Discussion

In this study, we investigated the track-specific and regional fiber tractography of advanced jazz improvisers and compared the findings with a control group of nonmusicians. We analyzed the anisotropic diffusion properties GFA and NQA for fibers crossing in previously

defined brain regions and the underlying fiber pathways connecting them. We found the region-based fiber crossings and the underlying white matter pathways in advanced improvisers characterized by higher fiber integrity (NQA), especially in the frontal motor regions and the connecting fiber pathways as compared to nonmusicians. When we checked the consistency of the functional interaction pattern of information flow from dlPFC to SMA during task performance, with the underlying fiber pathways connecting dlPFC and SMA, we found the dlPFC-SMA fiber pathway in advanced improvisers is enhanced with higher NQA measures compared to nonmusicians. These results suggest the white matter fiber properties have behavioral consequences that reflect the functional architecture of creative expertise. On the other hand, we found no significant differences in GFA measures in the frontal motor regions and the connecting fiber pathways as compared to nonmusicians.

Previous DTI studies of musicians have mainly discussed the diffusion properties of the underlying white matter microstructure in terms of FA using the probabilistic tractography methods. Most of the studies have tended to use the long-range white matter tracts or literature driven brain regions as their regions of interest. However, these studies have yielded somewhat inconsistent findings, as some report high FA values [112-114] and other reports low FA values [115, 116] in musicians and other creative individuals (for a review, see Moore 2014 [102]). Such inconsistency may be due to several factors including, methods, types of musicians, experience, expertise level, training, skills, and creative potential. In this study, we examined the NQA instead of FA using the deterministic fiber tractography, the Q-Space diffeomorphic reconstruction (QSDR) approach [27, 44], which calculates the density distribution of water diffusion at different orientations. We also examined GFA using the same deterministic QSDR method, which is similar to FA. But, the NQA measure used in this study is different than the

traditionally used fractional anisotropy (FA). QA is reported to have lower susceptibility to partial volume effects of crossing fibers and free-water, resulting in a better resolution with QA-aided tractography, which outperforms the FA-aided tractography [28, 44]. Since QA is sensitive to the compactness of the fiber bundle, the normalization of QA (NQA) reduces the variability resulting in stabilizing the spin-density measurement across subjects. On the other hand, generalized FA (GFA) suffers from the same partial volume effect as FA, and its value decreases in fiber crossing or voxels with partial volume effect [27, 28].

We found significantly higher NQA in several brain regions of advanced improvisers compared to nonmusicians, specifically in dlPFC in IFG, lPMC in MFG, both of which were associated with higher node activity during musical improvisation [100]. In addition, the fiber pathways connecting these regions are characterized by higher NQA, specifically the fiber pathways between the frontal (dlPFC) and motor regions (lPMC & SMA). NQA in the fiber pathway between dlPFC and SMA, the connection associated with the information flow during musical improvisation, is significantly higher in advanced improvisers compared to nonmusicians, suggesting that the underlying fiber integrity may serve as the basis for functional connectivity. On the other hand, we found no significant differences in regional GFA measures and the connecting fiber pathways in jazz improvisers as compared to nonmusicians in the frontal motor regions (dlPFC, lPMC & SMA) and fiber pathways connecting these regions.

Cognitive processes underpinning musical improvisation include fitting responses to an overall architectural structure, first selecting individual auditory and motor chunks, and then combining these chunks into an action chain [45, 64]. The areas that exhibited increased activation during improvisation in our previous study were dlPFC, lPMC, SMA, and RCb [100]. The dlPFC is associated with goal-directed behaviors that are consciously monitored, evaluated,

and corrected and is a central part of the executive control network (ECN). Specifically, dlPFC is involved in inhibiting habitual responses [117]. The involvement of left dlPFC during musical tasks presumably indicates topdown control, attentional monitoring, and evaluation [60, 118]. The activation of the motor planning areas lPMC in MFG and SMA during improvisation may be due to the process of selecting single motor acts or single sensorimotor associations associated with the hierarchical organization of the human behaviors [50].

Concerning the connectivity between ECN and motor regions, the elevated white matter fiber anisotropy of these regional crossings in advanced jazz improvisers may underline the increased performance and activity during creative cognition, working memory tasks, practice, and training [113, 119, 120]. Further, the enhanced frontal-motor fiber pathways characterized by higher NQA may be due to these behaviors. Although there was less causal effect during improvisation compared to pre-learned conditions, net information flow is always from dlPFC to SMA in both conditions. The structural connectivity of the advanced jazz improvisers may subserve as the basis for their functional interaction during musical tasks. With the highly enhanced underlying white matter fiber pathways, the output of the executive network evaluation may need minimal communication to motor regions during real-time musical improvisation compared to prelearned performance. In other words, enhanced fiber tracts in experts may subserve as the basis of efficient execution of their overlearned skills and strategies when it comes to creating seemingly novel feats.

There are several limitations to this study. First, NQA measures yielded significant findings compared to the GFA measures, but unfortunately, there is no way to assert the accuracy of tractography. However, it is noteworthy that NQA-aided tractography has been shown to be a better approach for examining fiber properties, which can filter out noisy fiber

tracts and yield results in a higher spatial resolution due to its lower susceptibility to partial volume effects [28]. The goal here was to compare the differences between expert jazz improvisers and control nonmusicians and explore the underlying white matter architecture associated with the functional states during task execution, but future work would benefit from comparing the samples of experts from different creative domains and analyze the whole brain architecture. Further, expanding the investigations in other creative domains like literary creativity, drawing creativity, dance, etc. might extend the understanding of the structural organization in domain-specific and domain-general creativity.

4.6 Conclusion

In this study, we investigated the white matter fiber properties of advanced jazz improvisers by conducting the QSDR deterministic tractography analysis. The elevated NQA measures in advanced jazz improvisers indicate enhanced task-supportive structural connectivity in improvisers compared to nonmusicians. The enhanced white matter fiber architecture in advanced jazz improvisers is consistent with the frontal to supplementary motor functional connectivity, which altogether points to the neural basis of expert's real-time creative performance.

5 SUMMARY

The present dissertation investigated the brain functional and structural basis of musical creativity of advanced level jazz improvisers using functional MRI and diffusion MRI methods. In the functional MRI study, we examined brain activity and connectivity during improvisation and compared the findings with the pre-learned condition. In the diffusion MRI study, we

explored track-specific and region-based white matter fiber properties of advanced jazz improvisers and compared the results with nonmusicians.

In the functional MRI investigation, the activation analysis showed musical improvisation compared with prelearned melody is characterized by significantly higher activity in left inferior frontal gyrus (IFG) that included the Broca's area (BCA), dorsolateral prefrontal cortex (dlPFC), motor areas, lateral premotor cortex (lPMC) in middle frontal gyrus (MFG), and left supplementary motor area (SMA) plus the right cerebellum (RCb). The cross-correlation analysis revealed the functionally correlated connections between these activated regions, higher functional connectivity during the pre-learned condition, both in number and strength, compared to improvisation. Further, using Granger causality analysis, we discovered the information flow pattern during the functional states of improvisatory and pre-learned conditions. Whether it is the pre-learned or improvised condition, there is a causal flow from lateral prefrontal regions to motor areas, especially from the dorsolateral prefrontal cortex (dlPFC) to supplementary motor areas (SMA), and the strength is higher during pre-learned condition compared to improvisation. Most of the previous studies revealed the involvement of almost all of the lateral prefrontal, frontal, and motor regions during creative tasks but with varying network interaction patterns [3, 46, 61-64, 99, 103, 117, 118, 121-131]. The inconsistent connectivity pattern might be due to the diverse expertise level and the level of cognitive demand during production, memory retrieval, information processing, and task execution in real-time. Jazz improvisation being one of the complex forms of musical creativity, overall brain activity, and connectivity pattern along with the structural changes [103, 113, 132-137], depends on participants' expertise level, skills, and knowledge.

In diffusion-weighted MRI, the fiber tractography analysis revealed enhanced track-specific and regional white matter fiber integrity in advanced jazz improvisers compared to nonmusicians. Specifically, there was a higher normalized quantitative anisotropy in the lateral prefrontal cortex and the supplementary motor area. Using the connectivity measurement, we further discovered the white matter structure of advanced jazz improvisers, the enhanced fiber pathways connecting the dlPFC and SMA characterized by higher NQA compared to nonmusicians. The elevated NQA measures in advanced jazz improvisers indicate enhanced task-supportive structural connectivity in improvisers compared to nonmusicians. The enhanced white matter fiber architecture in advanced jazz improvisers is consistent with the frontal to supplementary motor functional connectivity, which altogether points to the neural basis of expert's real-time creative performance. These results point to the notion that an expert's performance under real-time constraints is an internally directed behavior controlled primarily by a smaller brain network, that has enhanced task-supportive structural connectivity. Overall, these findings suggest that a creative act of an expert is functionally controlled by a smaller cortical network as in any internally directed attention and is encapsulated by the long-timescale brain structural network changes in support of the related cognitive underpinnings.

As a primary interest, our fMRI research mainly focused on a functional network consisting of brain regions involved in real-time creative behavior (musical improvisation). We observed a divergent activity and connectivity pattern (higher activity with less functional connectivity) during improvisation, which we think has a strong neurophysiological basis of blood-oxygenation dependent (BOLD) fMRI origin. The regional BOLD response can be attributed to the synaptic input to the local neuronal population and its intrinsic processing [11, 12] that dominantly contributes to the overall activity (up to approximately 79%) [87].

Consistent with these findings, it is reasonable to assume that the ongoing cognitive load is fulfilled by undergoing regional intrinsic neural processing resulting in elevated regional activity rather than greater coordination among activated regions. On the other hand, the participants in our study, who were expert improvisers with extended knowledge of the dictated harmonic context, the improvisatory performances benefit from associative bottom-up processes [138] thus might be resulting in the attenuated executive control (ECN). We didn't see such divergent activity and connectivity patterns explored in musical creativity (improvisation) literature. Future studies should investigate whether and how such patterns exist or vary across domain-specific or general creative behaviors and whether such patterns vary in participants with different levels of expertise.

Our functional connectivity analysis was mainly based on a specific network of brain regions characterized by higher activity during musical improvisation compared to prelearned condition. The brain regions with significantly higher activation are mostly localized in the left hemisphere, which includes the dorsolateral prefrontal cortex (dlPFC), lateral premotor cortex(lPMC), left supplementary area (SMA), Broca's Area (BCA) in left inferior frontal gyrus (IFG). Such a left-lateralized activity pattern in experts aligns with the left-hemispheric dominance for internalized tasks, context-dependent habituated behaviors, and processing [138, 139]. One of the brain regions that we were expecting to see involved during improvisation was left medial prefrontal region of default mode network (DMN), whose role is explained in the generation of improvised output without conscious involvement in a study of six professional pianists where they played a 35-note keyboard [61]. In this case, the DMN may have been able to guide improvisational choices due to the high level of improvisational training of the participants. Whereas in another study by Donnay et al. (2014) [62] that included expert

improvisers, increased activation in frontal control regions is reported, which may be due to the extra cognitive resources related to interpreting and responding to another musician during improvisation may be responsible for the activation related to the ECN. One should note that the regional brain activation may vary in strength and number by changing the level of significance and clustering threshold during brain activation analysis, which might influence the network level activity and connectivity pattern. The recent improvisation studies are leaning towards exploring the whole brain dynamics, has explored the involvement of other brain network like salience network, language network in dynamic interplay of the DMN and ECN [137, 140]. Currently, we are extending our network connectivity analysis further to explore the whole brain connectivity dynamics during the constrained, prelearned condition and the free, spontaneous improvisation in real-time.

Although the contemporary research findings suggest some common and distinct activations patterns across domain-specific and domain-general creative behaviors, including music, drawing, dance, and writing [3], how the individual creative ability, expertise, and quality of improvisation influence the neurocognitive dynamics is not clearly understood. Recent SPM-EEG study of jazz guitarist [138] explored the dual-process model of creativity depending upon the dominance and relaxation of the ECN. High-quality improvisations were characterized by left frontal-lobe processing, whereas the right hemispheric processing was associated with less creative improvisation [138]. Even though we have rated the vocalized audio files (both improvised and prelearned melodies) in our study, performances were not rated for the quality, but instead, were rated for accuracy using the Consensual Assessment Technique [85]. Accuracy for the improvisation trials was defined as “pitches imply underlying blues chord progression and rhythms imply a steady pulse.” We should note that due to technical difficulties, we only

recorded the audio from 13 participants though vocalizations were monitored during the data acquisition.

In our fMRI study, we incorporated musical imagery, and vocalization task instead of play condition to avoid any possible motor confounds during musical improvisation. Even without actual play tasks, we found significantly higher activations in premotor and supplementary motor areas (lPMC & SMA), and cerebellum, instead of the primary motor cortex. Further, the network interaction pattern, unidirectional information flow from dlPFC to SMA, and lPMC to SMA adds new insights of action-planning and motor sequencing in real-time musical creativity, which aligns with the Bashwiner's musical creativity motor system (MCMS) model [141]. The activation of left dlPFC during improvisation may indicate top-down control, attentional monitoring, and evaluation, which are consistent with previous studies and consistent with functions of the ECN [47, 60].

Our diffusion MRI investigation was primarily focused on the track-specific and region-based tractography analysis based on the functional network of brain areas and their connections explored in our function MRI investigations. We mainly explored the anisotropic diffusion of white matter fiber tracts in terms of Quantitive Anisotropy (NQA), which is calculated from the peak fiber orientations on a spin distribution function [27]. The normalized QA measures in white matter fiber tracts of regions in the lateral prefrontal cortex (dlPFC & lPMC) and connecting pathways to the supplementary motor area (SMA) were elevated in expert improvisers which indicate the enhanced task-supportive frontal-motor structural pathways in improvisers. Such consistency between the functional and structural networks reflect the specifc brain-behavior architecture of musical improvisation. Future analysis should be directed towards the whole-brain connectivity and network dynamics.

REFERENCES

1. Bilalić, M., *The neuroscience of expertise*. Cambridge fundamentals of neuroscience in psychology. 2017, Cambridge ; New York, NY: Cambridge University Press. xvi, 300 pages.
2. Hassin, R.R., et al., *Implicit working memory.* Conscious Cogn, 2009. **18**(3): p. 665-78.
3. Chen, Q., R.E. Beaty, and J. Qiu, *Mapping the artistic brain: Common and distinct neural activations associated with musical, drawing, and literary creativity.* Hum Brain Mapp, 2020.
4. Herculano-Houzel, S., *The human brain in numbers: a linearly scaled-up primate brain.* Frontiers in Human Neuroscience, 2009. **3**(31).
5. Ermentrout, B., *Neural networks as spatio-temporal pattern-forming systems.* Reports on Progress in Physics, 1998. **61**(4): p. 353-430.
6. Koch, C., *Biophysics of Computation: Information Processing in Single Neurons* Oxford University Press, New York., 1999.
7. Fields, R.D., *A new mechanism of nervous system plasticity: activity-dependent myelination.* Nat Rev Neurosci, 2015. **16**(12): p. 756-67.
8. Weishaput, D., V.D. Kochli, and B. Marincek, *How does MRI work?: An Introduction to the Physics and Function of Magnetic Resonance Imaging.* Springer Science and Business Media, Berlin, 2nd edition., 2006.
9. Cleary, J.O.S.H. and A.R. Guimarães, *Magnetic Resonance Imaging*, in *Pathobiology of Human Disease*, L.M. McManus and R.N. Mitchell, Editors. 2014, Academic Press: San Diego. p. 3987-4004.
10. Ogawa, S., et al., *Oxygenation-sensitive contrast in magnetic resonance image of rodent brain at high magnetic fields.* Magnetic resonance in medicine, 1990. **14 1**: p. 68-78.
11. Logothetis, N.K., *The Underpinnings of the BOLD Functional Magnetic Resonance Imaging Signal.* J Neurosci., 2003. **23**(10): p. 3963-3971.
12. Lauritzen, M., *Reading vascular changes in brain imaging: is dendrotic calcium the key?* Nat Rev Neurosci, 2005. **6**(1): p. 77-85.
13. Gore, J.C., *Principles and practice of functional MRI of the human brain.* The Journal of Clinical Investigation, 2003. **112**(1): p. 4-9.
14. Pierpaoli, C., Jezzard, P., Basser, P.J., Barnett, A., Chiro, G.Di.,, *Diffusion tensor MR imaging of the human brain.* Radiology, 1996. **201**(3): p. 637-648.
15. Basser, P.J., Mattiello, J., Lebihan, D., *Estimation of the Effective Self-Diffusion Tensor from the NMR Spin Echo.* Journal of Magnetic Resonance, Series B, 1994. **103**(3): p. 247-254.
16. Basser, P.J., J. Mattiello, and D. LeBihan, *MR diffusion tensor spectroscopy and imaging.* Biophys J, 1994. **66**(1): p. 259-67.
17. Le Bihan, D., et al., *MR imaging of intravoxel incoherent motions: application to diffusion and perfusion in neurologic disorders.* Radiology, 1986. **161**(2): p. 401-7.
18. Stejskal, E.O. and J.E. Tanner, *Spin diffusion measurements: spin echoes in the presence of a time-dependent field gradient.* The journal of chemical physics, 1965. **42**(1): p. 288-292.
19. Lauterbur, P.C., *Image Formation by Induced Local Interactions: Examples Employing Nuclear Magnetic Resonance.* Nature, 1973. **242**(5394): p. 190-191.

20. Emsell, L., W. Van Hecke, and J. Tournier, *Introduction to Diffusion Tensor Imaging. In: Van Hecke W., Emsell L., Sunaert S. (eds) Diffusion Tensor Imaging.* Springer, New York, NY, 2016.
21. Behrens, T.E., et al., *Probabilistic diffusion tractography with multiple fibre orientations: What can we gain?* Neuroimage, 2007. **34**(1): p. 144-55.
22. Behrens, T.E., et al., *Characterization and propagation of uncertainty in diffusion-weighted MR imaging.* Magn Reson Med, 2003. **50**(5): p. 1077-88.
23. Basser, P.J. and C. Pierpaoli, *Microstructural and Physiological Features of Tissues Elucidated by Quantitative-Diffusion-Tensor MRI.* Journal of Magnetic Resonance, Series B, 1996. **111**(3): p. 209-219.
24. Tuch, D.S., *Q-ball imaging.* Magn Reson Med, 2004. **52**(6): p. 1358-72.
25. Alexander, A.L., et al., *Diffusion tensor imaging of the brain.* Neurotherapeutics, 2007. **4**(3): p. 316-329.
26. Tournier, J.D., et al., *Resolving crossing fibres using constrained spherical deconvolution: Validation using diffusion-weighted imaging phantom data.* NeuroImage, 2008. **42**(2): p. 617-625.
27. Yeh, F.C., V.J. Wedeen, and W.Y. Tseng, *Generalized q-sampling imaging.* IEEE Trans Med Imaging, 2010. **29**(9): p. 1626-35.
28. Yeh, F.C., et al., *Deterministic diffusion fiber tracking improved by quantitative anisotropy.* PLoS One, 2013. **8**(11): p. e80713.
29. Ozarslan, E. and T.H. Mareci, *Generalized diffusion tensor imaging and analytical relationships between diffusion tensor imaging and high angular resolution diffusion imaging.* Magn Reson Med, 2003. **50**(5): p. 955-65.
30. Tournier, J.D., S. Mori, and A. Leemans, *Diffusion tensor imaging and beyond.* Magn Reson Med, 2011. **65**(6): p. 1532-56.
31. Smith, S.M., et al., *Tract-based spatial statistics: voxelwise analysis of multi-subject diffusion data.* Neuroimage, 2006. **31**(4): p. 1487-505.
32. Granger, C.W.J., *Investigating Causal Relations by Econometric Models and Cross-spectral Methods.* Econometrica, 1969. **37**(3): p. 424-438.
33. Friston, K.J., L. Harrison, and W. Penny, *Dynamic causal modelling.* NeuroImage, 2003. **19**(4): p. 1273-1302.
34. Wiener, N., *The theory of prediction* Modern Mathematics for Engineers, McGrawHill, NY, 1956. **165**.
35. Dhamala, M., G. Rangarajan, and M. Ding, *Analyzing information flow in brain networks with nonparametric Granger causality.* NeuroImage, 2008. **41**(2): p. 354-362.
36. Dhamala, M., G. Rangarajan, and M. Ding, *Estimating Granger Causality from Fourier and Wavelet Transforms of Time Series Data.* Physical Review Letters, 2008. **100**(1): p. 018701.
37. Ding, M., Y. Chen, and S.L. Bressler, *Granger Causality: Basic Theory and Application to Neuroscience.* 2006.
38. Tuch, D.S., et al., *High angular resolution diffusion imaging reveals intravoxel white matter fiber heterogeneity.* Magn Reson Med, 2002. **48**(4): p. 577-82.
39. Zhang, H., et al., *NODDI: practical in vivo neurite orientation dispersion and density imaging of the human brain.* Neuroimage, 2012. **61**(4): p. 1000-16.
40. Parker, G.D., et al., *A pitfall in the reconstruction of fibre ODFs using spherical deconvolution of diffusion MRI data.* NeuroImage, 2013. **65**: p. 433-448.

41. Schilling, K., et al., *Comparison of 3D orientation distribution functions measured with confocal microscopy and diffusion MRI.* Neuroimage, 2016. **129**: p. 185-197.
42. Yeh, F.C. and T.D. Verstynen, *Converting Multi-Shell and Diffusion Spectrum Imaging to High Angular Resolution Diffusion Imaging.* Front Neurosci, 2016. **10**: p. 418.
43. Kuo, L.W., et al., *Diffusion spectrum MRI using body-centered-cubic and half-sphere sampling schemes.* J Neurosci Methods, 2013. **212**(1): p. 143-55.
44. Yeh, F.C. and W.Y. Tseng, *NTU-90: a high angular resolution brain atlas constructed by q-space diffeomorphic reconstruction.* Neuroimage, 2011. **58**(1): p. 91-9.
45. Pressing, J., *Improvisation: Methods and model*. 1988: Generative Processes in Music, Oxford.
46. Beaty, R.E., et al., *Creative Cognition and Brain Network Dynamics.* Trends Cogn Sci, 2016. **20**(2): p. 87-95.
47. Beaty, R.E., *The neuroscience of musical improvisation.* Neurosci Biobehav Rev., 2015. **51**: p. 108-117.
48. Beaty, R.E., et al., *Creative Cognition and Brain Network Dynamics.* Trends Cogn Sci., 2016. **20**(2): p. 87-95.
49. Jackendoff, R. and F. Lerdahl, *The capacity for music : What is it , and what ' s special about it ? Cognition, . http://doi.org/10.1016/j.cognition..11.005*. Vol. 100 SRC - GoogleScholar. 2005. 33-72.
50. Koechlin, E. and T. Jubault, *Broca's Area and the Hierarchical Organization of Human Behavior.* Neuron, 2006. **50**: p. 963-974.
51. Alamia, A., et al., *Disruption of Broca's Area Alters Higher-order Chunking Processing during Perceptual Sequence Learning.* Journal of Cognitive Neuroscience, 2016. **28**(3): p. 402-417.
52. Berliner, P.F., *Thinking in jazz.* University Of Chicago Press, 1994.
53. Norgaard, M., *Descriptions of improvisational thinking by artist-level jazz musicians.* Journal of Research in Music Education, 2011. **59**(2): p. 109-127.
54. Hay, J.F., et al., *Linking sounds to meanings: Infant statistical learning in a natural language*. Vol. 63. 2011. 93-106.
55. Brattico, E., B. Bogert, and T. Jacobsen, *Toward a Neural Chronometry for the Aesthetic Experience of Music.* Frontiers in Psychology, 2013. **4**(206).
56. Salimpoor, V.N., et al., *Predictions and the brain: how musical sounds become rewarding.* Trends Cogn Sci., 2015. **19**: p. 86-91.
57. Pearce, M.T. and G. Wiggins, *Auditory expectation: the information dynamics of music perception and cognition.* Top Cogn Sci., 2012. **4**: p. 625-52.
58. Norgaard, M., *How jazz musicians improvise: The central role of auditory and motor patterns.* Music Percept., 2014. **31**: p. 271-287.
59. Norgaard, M., et al., *Creating under pressure: Effects of divided attention on the improvised output of skilled jazz pianists.* Music Percept., 2016. **33**(5 SRC - GoogleScholar): p. 561-570.
60. Berkowitz, A.L. and D. Ansari, *Generation of novel motor sequences: the neural correlates of musical improvisation.* Neuroimage, 2008. **41**(2): p. 535-43.
61. Limb, C.J. and A.R. Braun, *Neural substrates of spontaneous musical performance: an FMRI study of jazz improvisation.* PLoS One, 2008. **3**(2): p. e1679.
62. Donnay, G.F., et al., *Neural substrates of interactive musical improvisation: an FMRI study of 'trading fours' in jazz.* PLoS One, 2014. **9**(2): p. e88665.

63. de Manzano, O. and F. Ullén, *Goal-independent mechanisms for free response generation: Creative and pseudo-random performance share neural substrates.* NeuroImage, 2012. **59**(1): p. 772-780.
64. Pinho, A.L., et al., *Addressing a Paradox: Dual Strategies for Creative Performance in Introspective and Extrospective Networks.* Cereb Cortex, 2016. **26**(7): p. 3052-63.
65. Zatorre, R.J., et al., *Hearing in the Mind's Ear: A PET Investigation of Musaical Imagery and Perception.* J Cogn Neurosci, 1996. **8**: p. 29-46.
66. Yumoto, M., et al., *Auditory imagery mismatch negativity elicited in musicians.* NeuroReport 2005. **16**: p. 1175-1178.
67. Kraemer, D.J., et al., *Musical imagery: sound of silence activates auditory cortex.* Nature, 2005. **434**(7030): p. 158.
68. Meister, I.G., et al., *Playing piano in the mind--an fMRI study on music imagery and performance in pianists.* Brain Res Cogn Brain Res, 2004. **19**(3): p. 219-28.
69. Lahav, A., E. Saltzman, and G. Schlaug, *Action Representation of Sound : Audiomotor Recognition Network While Listening to Newly Acquired Actions.* J Neurosci., 2007. **27**: p. 308-314.
70. Keller, P.E., *Mental imagery in music performance: underlying mechanisms and potential benefits*. Vol. 1252 SRC - GoogleScholar. 2011. 206-13.
71. Adhikari, B.M., et al., *The Brain Network Underpinning Novel Melody Creation.* Brain Connect, 2016. **6**(10): p. 772-785.
72. Friston, K.J., et al., *Statistical parametric maps in functional imaging: a general linear approach.* Hum. Brain Mapp., 1995. **2**: p. 189-210.
73. Bond, C. and K. Richardson, *Seeing the Fisher z-transformation.* Psychometrika, 2004. **69**: p. 291–303.
74. Cox, N., *Speaking stata: correlation with confidence, or Fisher's z revisited.* Stata J 2008. **8**: p. 413–439.
75. Silver, N. and W. Dunlap, *Averaging correlation coefficients: Should Fisher's z transformation be used?* Journal of Applied Psychology, 1987. **72(1)**: p. 146-148.
76. Aguirre, G.K., E. Zarahn, and M. D'Esposito, *The variability of human, BOLD hemodynamic responses.* Neuroimage, 1998. **8**: p. 360-369.
77. Handwerker, D.A., J.M. Ollinger, and M. D'Esposito, *Variation of BOLD hemodynamic responses across subjects and brain regions and their effects on statistical analyses.* Neuroimage, 2004. **21**(4): p. 1639-51.
78. David, O., et al., *Identifying neural drivers with functional MRI: an electrophysiological validation.* PLoS Biol, 2008. **6**(12): p. 2683-97.
79. Roebroeck, A., E. Formisano, and R. Goebel, *The identification of interacting networks in the brain using fMRI: Model selection, causality and deconvolution.* Neuroimage, 2011. **58**(2): p. 296-302.
80. Valdes-Sosa, P.A., et al., *Effective connectivity: influence, causality and biophysical modeling.* Neuroimage, 2011. **58**(2): p. 339-61.
81. Wu, G.R., et al., *A blind deconvolution approach to recover effective connectivity brain networks from resting state fMRI data.* Med Image Anal, 2013. **17**(3): p. 365-74.
82. Dhamala, M., G. Rangarajan, and M. Ding, *Analyzing information flow in brain networks with nonparametric Granger causality.* Neuroimage, 2008. **41**(2): p. 354-62.
83. Blair, R.C. and W. Karniski, *An alternative method for significance testing of waveform difference potentials.* Psychophysiology, 1993. **30**: p. 518-524.

84. Brovelli, A., et al., *Beta oscillations in a large-scale sensorimotor cortical network: directional influences revealed by Granger causality.* Proc. Natl. Acad. Sci. U S A, 2004. **101**(26): p. 9849-54.
85. Amabile, T.M., *Creativity in context*. 1996: Boulder, CO: Westview Press.
86. Jarvinen, T., *Tonal Hierarchies in Jazz Improvisation.* Music Perception, 1995. **12**(4): p. 415-437.
87. Harris, S., et al., *Does Neural Input or Processing Play a Greater Role in the Magnitude of Neuroimaging Signals?* Front Neuroenergetics, 2010. **2**: p. 15.
88. Kleinmintz, O.M., et al., *Participation of the left inferior frontal gyrus in human originality.* Brain Struct Funct, 2017.
89. Norgaard, M., *Descriptions of improvisational thinking by artist-level jazz musicians*. Vol. 59. 2011. 109-127.
90. Liu, S., et al., *Brain activity and connectivity during poetry composition: Toward a multidimensional model of the creative process. .* Hum Brain Mapp. https://doi.org/10.1002/hbm.22849, 2015.
91. Ellamil, M., et al., *Evaluative and generative modes of thought during the creative process.* NeuroImage, 2012. **59**(2): p. 1783-1794.
92. Levelt, W.J., *Spoken word production: a theory of lexical access.* Proc Natl Acad Sci U S A, 2001. **98**(23): p. 13464-71.
93. Flinker, A., et al., *Redefining the role of Broca's area in speech.* Proc Natl Acad Sci U S A, 2015. **112**(9): p. 2871-5.
94. Baumann, S., et al., *A network for audio-motor coordination in skilled pianists and non-musicians.* Brain Res, 2007. **1161**: p. 65-78.
95. Goldman, A., *Towards a cognitive–scientific research program for improvisation: Theory and an experiment.* Psychomusicology: Music, Mind, and Brain, 2013. **23**(4): p. 210-221.
96. Buhusi, C.V. and W.H. Meck, *What makes us tick? Functional and neural mechanisms of interval timing.* Nat Rev Neurosci, 2005. **6**(10): p. 755-65.
97. Spencer, R.M.C., R.B. Ivry, and H.N. Zelaznik, *Role of the cerebellum in movements: control of timing or movement transitions?* Experimental Brain Research, 2005. **161**(3): p. 383-396.
98. Schaefer, R.S., et al., *Moving to music: effects of heard and imagined musical cues on movement-related brain activity.* Front Hum Neurosci., 2014. **8**: p. 774.
99. Faber, S.E.M. and A.R. McIntosh, *Towards a standard model of musical improvisation.* Eur J Neurosci, 2019.
100. Dhakal, K., et al., *Higher Node Activity with Less Functional Connectivity During Musical Improvisation.* Brain Connect, 2019. **9**(3): p. 296-309.
101. Dietrich, A., *The cognitive neuroscience of creativity.* Psychonomic Bulletin & Review, 2004. **11**(6): p. 1011-1026.
102. Moore, E., et al., *Can musical training influence brain connectivity? Evidence from diffusion tensor MRI.* Brain Sci, 2014. **4**(2): p. 405-27.
103. Arkin, C., et al., *Gray Matter Correlates of Creativity in Musical Improvisation.* Front Hum Neurosci, 2019. **13**: p. 169.
104. Zamm, A., et al., *Pathways to seeing music: enhanced structural connectivity in colored-music synesthesia.* Neuroimage, 2013. **74**: p. 359-66.

105. Loui, P., H.C. Li, and G. Schlaug, *White matter integrity in right hemisphere predicts pitch-related grammar learning.* Neuroimage, 2011. **55**(2): p. 500-7.
106. Gaser, C. and G. Schlaug, *Brain Structures Differ between Musicians and Non-Musicians.* The Journal of Neuroscience, 2003. **23**(27): p. 9240-9245.
107. Roberts, R.E., E.J. Anderson, and M. Husain, *White matter microstructure and cognitive function.* Neuroscientist, 2013. **19**(1): p. 8-15.
108. Scholz, J. and V.J.-B. Tomassini, H, *Individual Differences in White Matter Microstructure in the Healthy Brain*. Diffusion MRI - From Quantitative Measurement to In vivo Neuroanatomy, ed. H. Johansen-Berg and T.E.J. Behrens. 2009: Elsevier Inc. 502.
109. Fritzsche, K.H., et al., *Opportunities and pitfalls in the quantification of fiber integrity: what can we gain from Q-ball imaging?* NeuroImage, 2010. **51**(1): p. 242-251.
110. Yeh, F.C., et al., *Differential tractography as a track-based biomarker for neuronal injury.* NeuroImage, 2019. **202**: p. 116131.
111. Yeh, F.C., et al., *Automatic Removal of False Connections in Diffusion MRI Tractography Using Topology-Informed Pruning (TIP).* Neurotherapeutics, 2019. **16**(1): p. 52-58.
112. Schmithorst, V.J. and M. Wilke, *Differences in white matter architecture between musicians and non-musicians: a diffusion tensor imaging study.* Neuroscience Letters, 2002. **321**(1): p. 57-60.
113. Bengtsson, S.L., et al., *Extensive piano practicing has regionally specific effects on white matter development.* Nat Neurosci, 2005. **8**(9): p. 1148-50.
114. Han, Y., et al., *Gray matter density and white matter integrity in pianists' brain: a combined structural and diffusion tensor MRI study.* Neurosci Lett, 2009. **459**(1): p. 3-6.
115. Halwani, G.F., et al., *Effects of practice and experience on the arcuate fasciculus: comparing singers, instrumentalists, and non-musicians.* Front Psychol, 2011. **2**: p. 156.
116. Imfeld, A., et al., *White matter plasticity in the corticospinal tract of musicians: a diffusion tensor imaging study.* Neuroimage, 2009. **46**(3): p. 600-7.
117. de Manzano, Ö. and F. Ullén, *Activation and connectivity patterns of the presupplementary and dorsal premotor areas during free improvisation of melodies and rhythms.* NeuroImage, 2012. **63**(1): p. 272-80.
118. Beaty, R.E., *The neuroscience of musical improvisation.* Neurosci Biobehav Rev, 2015. **51**: p. 108-17.
119. Wertz, C.J., et al., *White matter correlates of creative cognition in a normal cohort.* Neuroimage, 2020. **208**: p. 116293.
120. Takeuchi, H., et al., *Training of working memory impacts structural connectivity.* J Neurosci, 2010. **30**(9): p. 3297-303.
121. Beaty, R.E., P. Seli, and D.L. Schacter, *Network Neuroscience of Creative Cognition: Mapping Cognitive Mechanisms and Individual Differences in the Creative Brain.* Curr Opin Behav Sci, 2019. **27**: p. 22-30.
122. Madore, K.P., et al., *Neural Mechanisms of Episodic Retrieval Support Divergent Creative Thinking.* Cereb Cortex, 2019. **29**(1): p. 150-166.
123. Benedek, M., et al., *To create or to recall original ideas: Brain processes associated with the imagination of novel object uses.* Cortex, 2018. **99**: p. 93-102.
124. Bashwiner, D.M., et al., *Resting state functional connectivity underlying musical creativity.* Neuroimage, 2020. **218**: p. 116940.

125. López-gonzález, B.M., D. Ph, and C.J. Limb, *Musical Creativity and the Brain.* American Psychologist, 2012(February): p. 1-15.
126. Pinho, A.L., et al., *Connecting to create: expertise in musical improvisation is associated with increased functional connectivity between premotor and prefrontal areas.* J Neurosci, 2014. **34**(18): p. 6156-63.
127. Holm, L., et al., *Executive control and working memory are involved in sub-second repetitive motor timing.* Exp Brain Res, 2017. **235**(3): p. 787-798.
128. Ullen, F., M.A. Mosing, and G. Madison, *Associations between motor timing, music practice, and intelligence studied in a large sample of twins.* Ann N Y Acad Sci, 2015. **1337**: p. 125-9.
129. Mosing, M.A., et al., *Practice does not make perfect: no causal effect of music practice on music ability.* Psychol Sci, 2014. **25**(9): p. 1795-803.
130. Beaty, R.E., et al., *Brain networks of the imaginative mind: Dynamic functional connectivity of default and cognitive control networks relates to openness to experience.* Hum Brain Mapp, 2018. **39**(2): p. 811-821.
131. Palomar-García, M.-Á., et al., *Modulation of Functional Connectivity in Auditory–Motor Networks in Musicians Compared with Nonmusicians.* Cerebral Cortex, 2016: p. bhw120-bhw120.
132. Wesseldijk, L.W., F. Ullen, and M.A. Mosing, *The effects of playing music on mental health outcomes.* Sci Rep, 2019. **9**(1): p. 12606.
133. de Manzano, O. and F. Ullen, *Same Genes, Different Brains: Neuroanatomical Differences Between Monozygotic Twins Discordant for Musical Training.* Cereb Cortex, 2018. **28**(1): p. 387-394.
134. Ullen, F., D.Z. Hambrick, and M.A. Mosing, *Rethinking expertise: A multifactorial gene-environment interaction model of expert performance.* Psychol Bull, 2016. **142**(4): p. 427-46.
135. Loui, P., et al., *Musical Instrument Practice Predicts White Matter Microstructure and Cognitive Abilities in Childhood.* Front Psychol, 2019. **10**: p. 1198.
136. Loui, P., et al., *White Matter Correlates of Musical Anhedonia: Implications for Evolution of Music.* Front Psychol, 2017. **8**: p. 1664.
137. Bashwiner, D.M., et al., *Musical Creativity "Revealed" in Brain Structure: Interplay between Motor, Default Mode and Limbic Networks.* Scientific Reports, 2016. **6**(1): p. 20482.
138. Rosen, D.S., et al., *Dual-process contributions to creativity in jazz improvisations: An SPM-EEG study.* NeuroImage, 2020. **213**: p. 116632.
139. Goldberg, E., K. Podell, and M. Lovell, *Lateralization of frontal lobe functions and cognitive novelty.* J Neuropsychiatry Clin Neurosci, 1994. **6**(4): p. 371-8.
140. Alves Da Mota, P., et al., *The dynamics of the improvising brain: a study of musical creativity using jazz improvisation.* bioRxiv, 2020: p. 2020.01.29.924415.
141. Bashwiner, D. and D. Bacon, *Musical creativity and the motor system.* Current Opinion in Behavioral Sciences, 2019. **27**: p. 146-153.

APPENDICES

Appendix A

Appendix A.1

The vocalization trials were rated for accuracy independently by two expert jazz musicians not affiliated with the study using the Consensual Assessment Technique [85]. Accuracy was rated on a seven-point Likert Scale with 1 being “extremely inaccurate” and 7 being “highly accurate”. We analyzed the vocalized audio files of improvisation tasks of 13 participants and found out that the overall ratings were excellent. **Table A.1.1** and **Table A.1.2** includes the subject-wise and run-wise rating details for pre-learned and improvised vocalizations, respectively. We sorted their ratings in increasing values, divided 12 participants around the median rating into two groups (high-scoring group (HSG) and low scoring group (LSG)), and performed activation analyses of vocalized improvisation (VI) comparing these two groups. We compared VI_HSG minus VI_LSG and the other way around, and there is not any significant difference ($p < 0.0005$, uncorrected, and cluster extent $k > 20$) in brain activation either way. So, the little discrepancy during the performance does not reflect in cluster level activation in the brain during vocalized improvisation.

If we lower the threshold to a very low ($p < 0.01$, uncorrected and cluster extent $k > 5$), the activation at Brodmann area 40 (postcentral area, a part of Wernicke's area, language perception and processing) appears during VI_HSG compared to VI_LSG. There is no activation in the other way of contrast.

Thus, we do not think that the level of variability in accuracy that we have would affect the main results of brain activations.

Table A.1.1 Average ratings of improvised vocalization

Participant No.	Run 1	Run 2	Run 3	Average Rating
08	5.333	5.575	5.667	**5.6**
09	6.6	6.5	6.167	**6.409**
10	6	5.833	6.167	**6**
12	6.25	6.167	6	**6.136**
13	6.5	6	5.625	**6.045**
15	5.833	4.875	4.475	**5.091**
16	6.167	6	5	**5.889**
17	6.125	6	6	**6.05**
18	5.875	6	5.875	**5.917**
19	6.617	6.275	5.75	**6.122**
21	5.875	5.875	6	**5.917**
22	6.625	6.75	6.333	**6.591**
24	6.333	6.5	6.125	**6.3**

Table A.1.2 Average ratings of pre-learned vocalization

Participant No.	Run 1	Run 2	Run 3	Average Rating
08	6.838	6.15	6.25	**6.373**
09	7	6.75	6.333	**6.727**
10	6.5	6.625	6.5	**6.55**
12	6.125	6.375	6.25	**6.25**

13	6	6.25	6.375	**6.208**
15	5.75	6.125	6.375	**6.083**
16	6.875	6.5	6.667	**6.7**
17	6.5	6.333	6.625	**6.5**
18	5.5	5.375	5.375	**5.417**
19	6.75	6.625	6.5	**6.667**
21	6.25	6.625	6.375	**6.417**
22	6.5	6.875	6.875	**6.417**
24	6.333	6.5	5.625	**6.136**

Appendix A.2

We wanted to avoid potential confounds of overt movement in musical improvisation, unlike how it was done in previous studies (already discussed in vocalizing and imagery improvisation). For that, we introduced a new imagery task in our study: imagery improvisation and singing the pre-learned melody.

We further looked at brain activations results of contrasting the vocalized improvisation (VI) with the imagined improvisation (II) or vice-versa. The results are shown in **Figure A.2**; for II-VI, there is a higher activation in Brodmann area 19 (visual cortex) and Brodmann area 40 (postcentral area, a part of Wernicke's language area) and (ii) for VI-VII, there is an activation in BA 41 (auditory cortex) and precentral gyrus (motor area) as expected.

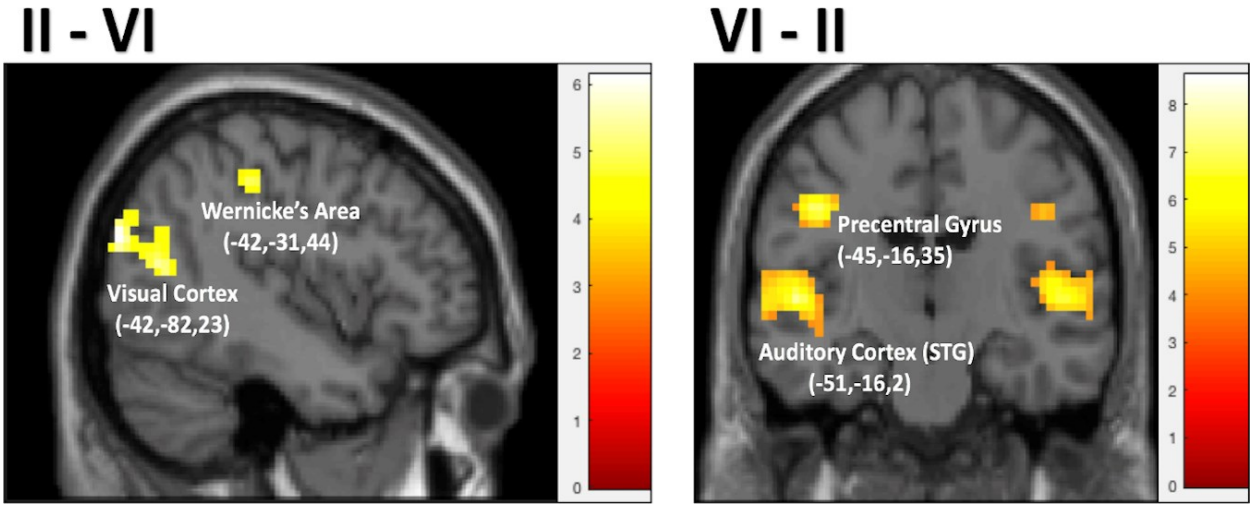

Figure A.1.1 Brain activations during imagery and vocalized condition

Left panel shows the brain activation during imagery improvised condition (II) versus vocalize improvised condition (VI), whereas the right panel shows the brain activation in other way, i.e., vocalize improvised condition (VI) versus imagery improvisation (II)

Appendix A.3

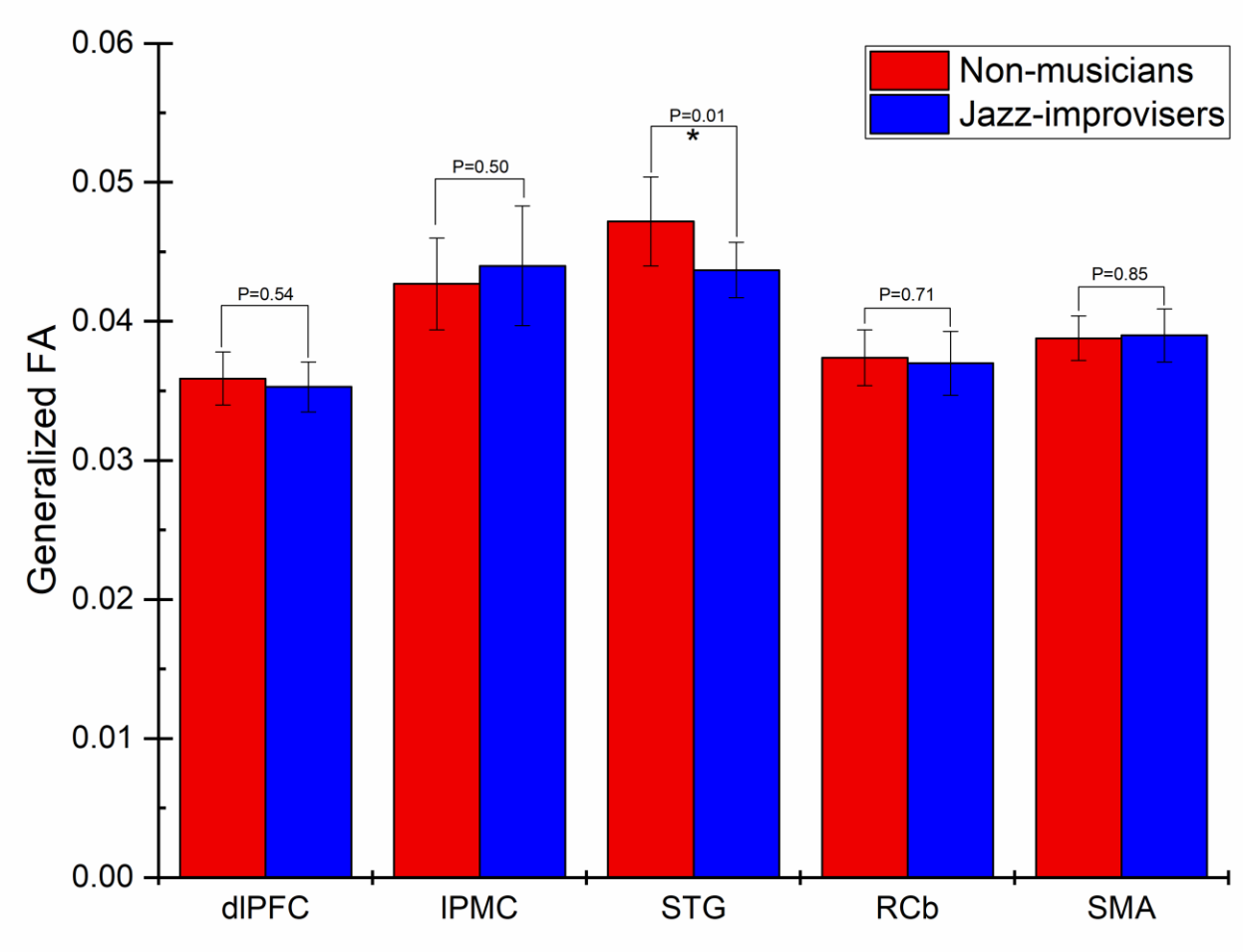

Figure A.1.2 Region-based generalized fractional anisotropy

Region-based subject-averaged generalized fractional anisotropy (GFA) for advanced jazz improvisers and control nonmusicians. No significant differences observed in regional GFA measures except in fiber crossing of STG.

Appendix A.4

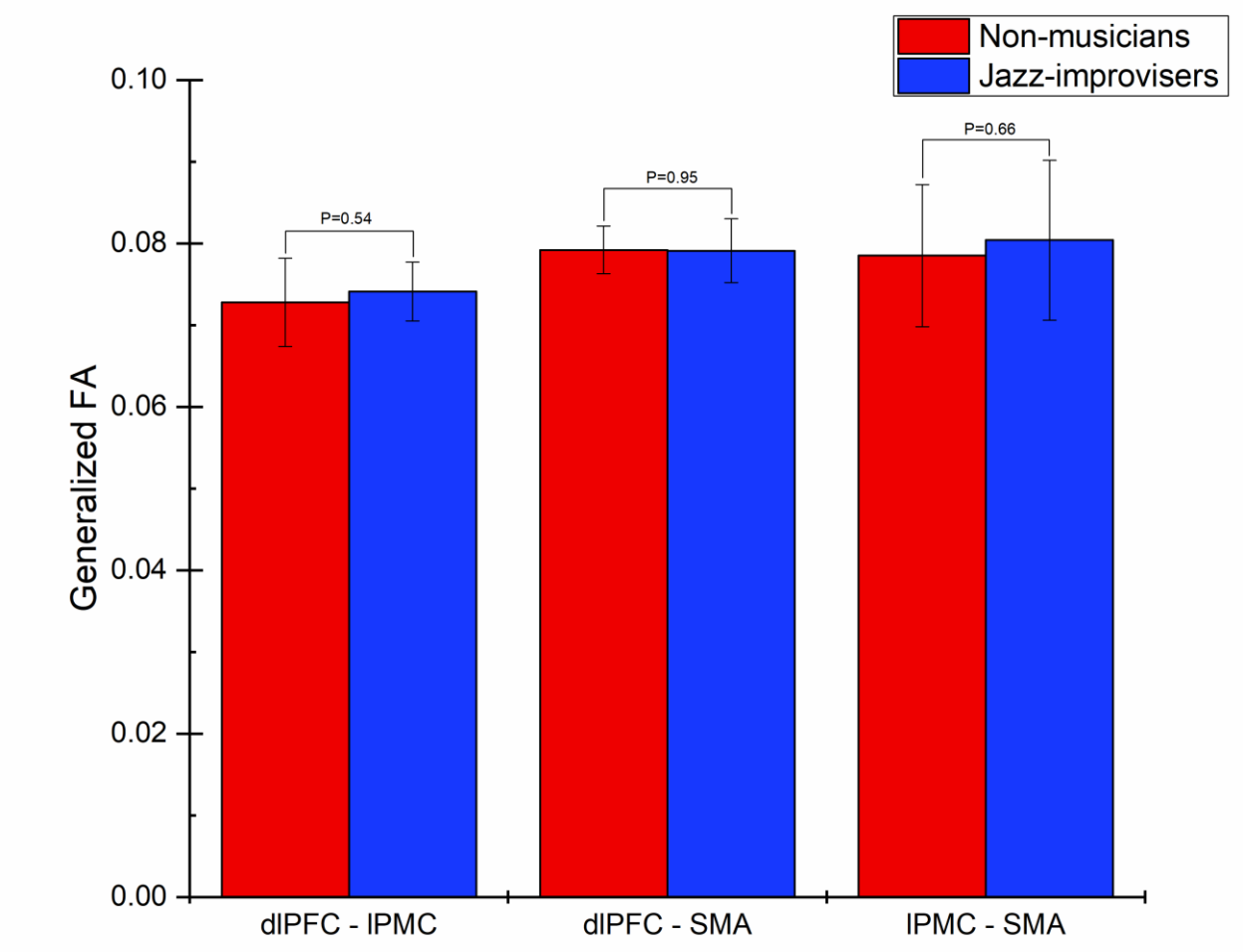

Figure A.1.3 Track-specific generalized fractional anisotropy

Track-specific subject-averaged generalized fractional anisotropy (GFA) for advanced jazz improvisers and nonmusicians. No significant differences were observed in GFA measures.